

**EPOXY/SINGLE WALLED CARBON NANOTUBE  
NANOCOMPOSITE THIN FILMS FOR COMPOSITES  
REINFORCEMENT**

A Thesis

by

GRAHAM LEICESTER WARREN

Submitted to the Office of Graduate Studies of  
Texas A&M University  
in partial fulfillment of the requirements for the degree of

MASTER OF SCIENCE

May 2009

Major Subject: Mechanical Engineering

**EPOXY/SINGLE WALLED CARBON NANOTUBE  
NANOCOMPOSITE THIN FILMS FOR COMPOSITES  
REINFORCEMENT**

A Thesis

by

GRAHAM LEICESTER WARREN

Submitted to the Office of Graduate Studies of  
Texas A&M University  
in partial fulfillment of the requirements for the degree of

MASTER OF SCIENCE

Approved by:

Chair of Committee,  
Committee Members,

Head of Department,

Hung-Jue Sue  
James Boyd  
Christian Schwartz  
Dennis O'Neal

May 2009

Major Subject: Mechanical Engineering

## ABSTRACT

Epoxy/Single Walled Carbon Nanotube Nanocomposite Thin Films  
for Composites Reinforcement. (May 2009)

Graham Leicester Warren, B.S., Texas A&M University

Chair of Advisory Committee: Dr. Hung-Jue Sue

This work is mainly focused upon the preparation, processing and evaluation of mechanical and material properties of epoxy/single walled carbon nanotube (SWCNT) nanocomposite thin films. B-staged epoxy/SWCNT nanocomposite thin films at 50% of cure have been prepared for improving conductivity and mechanical performance of laminated composites. The SWCNTs were functionalized by oxidation and subsequent grafting using polyamidoamine generation 0 dendrimers (PAMAM-G0). The epoxy nanocomposites containing SWCNTs were successfully cast into thin films by manipulating degree of cure and viscosity of epoxy.

The first section of this study focuses on the covalent oxidation and functionalization of single-walled carbon nanotubes (SWCNTs), which is necessary in order to obtain the full benefit of the SWCNTs inherent properties for reinforcement. In the second section of this work the preparation of B-staged epoxy/SWCNT nanocomposite thin films is discussed and what the purposes of thin films are. Additionally, the morphology as well as mechanical properties is evaluated by numerous means to obtain a clear picture as to the mechanisms of the epoxy/SWCNT

nanocomposites. Furthermore, the effects of using sulfanilamide as a more attractive surface modifier for improved dispersion and adhesion and the effects of nylon particles for improved toughening on epoxy/SWCNT nanocomposites are discussed which displays improvements in numerous areas.

Finally, based on these findings and previous studies, the B-staged epoxy/SWCNT nanocomposite thin films can be seamlessly integrated into laminated composite systems upon heating, and can serve as interleaves for improving conductivity and mechanical strengths of laminated fiber composite systems.

## DEDICATION

*I dedicate this work to the following people who have influenced my life:*

***My parents (David Warren and Julie Simpson) and brother (Kendall Warren) who have been supporting my dreams and aspirations throughout every aspect of my life.***

***Dr. Hung-Jue Sue** who has been providing me with the essential wisdom and fundamental knowledge to grow as a person and as a researcher.*

***Dr. Luyi Sun** whose academic enthusiasm and generous nature inspired me to further my education in the science and engineering field.*

***Dr. Woong-Jae Boo** who aided me in passing through various obstacles in my graduate career to help me become who I am today.*

## TABLE OF CONTENTS

		Page
ABSTRACT .....		iii
DEDICATION .....		v
TABLE OF CONTENTS .....		vi
CHAPTER		
I	INTRODUCTION.....	1
	Significance of Epoxy/SWCNT Thin Film Study.....	1
	Thesis Layout .....	7
II	COVALENT SURFACE OXIDATION AND FUNCTIONALIZATION OF SWCNTS: EFFECTS OF PAMAM-GO.....	8
	Experimental .....	8
	Results and Discussion.....	10
III	PREPARATION OF B-STAGED EPOXY/SWCNT NANOCOMPOSITE THIN FILMS FOR VARTM APPLICATIONS...	14
	Experimental .....	14
	Results and Discussion.....	16
IV	MORPHOLOGY OF EPOXY/SWCNT BASED NANOCOMPOSITES .....	22
	Experimental .....	22
	Results and Discussion.....	24
V	MECHANICAL PROPERTIES AND FRACTURE TOUGHNESS OF EPOXY/SWCNT BASED NANOCOMPOSITES.....	34

CHAPTER	Page
Experimental .....	34
Results and Discussion.....	36
VI EFFECT OF SULFANILAMIDE AND NYLON PARTICLES ON EPOXY/SWCNT BASED NANOCOMPOSITES .....	42
Experimental .....	42
Results and Discussion.....	43
VII CONCLUSIONS AND REMARKS .....	57
Conclusions on Epoxy/SWCNT Thin Film Study .....	57
Recommendations for Future Work.....	58
REFERENCES.....	59
VITA .....	64

## LIST OF FIGURES

FIGURE	Page
1 XPS spectra of oxidized SWCNT (O-SWCNT) .....	11
2 Schematic of functionalization of SWCNT by PAMAM-G0 .....	12
3 DSC thermograms of epoxy/SWCNT nanocomposite thin films .....	18
4 DSC thermograms of (a) 50% cured thin films, (b) 100% cured thin films.....	20
5 SEM images of fracture surface of nanocomposite samples.....	25
6 TEM image of epoxy/F-SWCNT .....	26
7 Optical image of $80 \times 80 \mu\text{m}^2$ area on the surface of an epoxy/P-SWCNT (0.5 wt%) nanocomposite thin film .....	29
8 Optical image of $80 \times 80 \mu\text{m}^2$ area on the surface of an epoxy/O-SWCNT (0.5 wt%) nanocomposite thin film.....	31
9 Optical image of $80 \times 80 \mu\text{m}^2$ area on the surface of an epoxy/F-SWCNT (0.5 wt%) nanocomposite thin film .....	33
10 Tensile curves of epoxy/SWCNT nanocomposites.....	37
11 DMA results of epoxy/nanocomposites .....	40
12 Chemical structure of sulfanilamide .....	43
13 OM images (10x) of F-SWCNT nanocomposite samples .....	47
14 Viscosity vs. shear rate of epoxy/nanocomposites .....	49
15 DMA results of epoxy/nylon nanocomposites .....	53
16 SEM images of fracture surface of neat epoxy nanocomposite samples.....	54

FIGURE	Page
17 SEM images of fracture surface of epoxy/F-SWCNT nanocomposite samples .....	55

## LIST OF TABLES

TABLE		Page
1	Required time to achieve a 50% B-stage cured thin film at 50 $\mu\text{m}$ thickness.....	19
2	Mechanical properties of bulk Epoxy/SWCNT nanocomposites (0.5 wt%) .....	36
3	Summary of key DMA properties .....	40
4	Glass transition temperature ( $T_g$ ) of Epoxy/SWCNT/Nylon nanocomposites .....	48
5	Mechanical properties of Epoxy/SWCNT nanocomposites (0.5 wt%) .....	50
6	Mechanical properties of Epoxy/SWCNT/Nylon nanocomposites (0.5 wt%) .....	51

# CHAPTER I

## INTRODUCTION

In this chapter, preliminary remarks are made to highlight the significance of studying epoxy/SWCNT nanocomposite thin films and review the development of this area in the past. Important factors and considerations which set the limitations of studying epoxy/SWCNT nanocomposite thin films are evaluated in detail to give an appreciation of the inherent complexity in its research. Finally, an outline is provided to lay out research components and the order which they will be evaluated upon in this thesis.

### **SIGNIFICANCE OF EPOXY/SWCNT THIN FILM STUDY**

Since their discovery [1], carbon nanotubes, especially single-walled carbon nanotubes (SWCNTs), have attracted significant interests due to their remarkable properties [2-5]. Among a wide range of applications, SWCNTs have been considered as an ideal reinforcing agent for composite applications [6] because of their superior Young's modulus ( $\sim 1$  TPa) [7] and high aspect ratio [8]. In addition to their extremely high modulus and strength, SWCNTs possess high electrical conductivity ( $>10^4$  S/cm) [9] and thermal conductivity ( $>2,000$  W/m·K) [10], which enable the preparation of

---

This thesis follows the style of *Journal of Applied Polymer Science*.

multifunctional high performance polymer composites. In recent years, SWCNT based polymer nanocomposites have been extensively studied through the uses of a wide range of polymer matrices [11-13] which include epoxy [14-16], polypropylene [17], polyethylene [18], poly(methyl methacrylate) [19], polyacrylonitrile [20] and poly(vinyl alcohol) [21], for various structural and functional applications.

In order to fully impart the unique properties of SWCNTs into polymers, it is critical to achieve: (1) good dispersion of SWCNTs in polymer matrices, (2) strong adhesion between SWCNTs and the matrix, and (3) alignment of SWCNTs [11,12]. Vast amounts of research efforts have been made to address the above needs, among which surface functionalization of SWCNTs is an attractive approach because it can address both the dispersion and adhesion attributes. Both covalent and noncovalent functionalization methods have been extensively studied and developed over the years [13]. Either method has its own advantages and disadvantages.

Because of the intrinsic van der Waals force attraction and high aspect ratio nature, SWCNTs are usually present in the form of bundles and ropes. Consequently, dispersion of SWCNTs in a media becomes a challenge. Especially, when they are mixed with a polymer, it will usually aggregate in polymer matrices. To be noted, when surface-functionalized SWCNTs are well dispersed in the polymer matrix, significant viscosity build-up is usually observed.

The poor dispersion of SWCNTs not only significantly lowers their efficiency as reinforcement but also causing SWCNTs to slip by each other when forces are applied to the composites [22]. Furthermore, poor adhesion between SWCNTs and most polymer

matrices is usually observed and is resulted from the atomically smooth non-reactive surface characteristics of SWCNTs. The lack of interfacial bonding limits the load transfer capability from matrix to SWCNTs. Typically, poorly adhered SWCNTs are pulled out of the matrix upon failure, thus limiting their reinforcement effect.

Tremendous research efforts have been made to address the above obstacles. For example, several approaches, such as ultrasonication, high shear mixing, use of surfactants, surface functionalization, encapsulation of SWCNTs and the combination of some of the above have been pursued [7,23]. Dispersion of SWCNTs in thermoplastics has been found to be more readily accomplished where shear mixing, stepwise dispersion, elongational flow mixing are effective. On the other hand, the dispersion of SWCNT in thermosets, such as epoxy, can be more challenging. Thus far, it has been shown that SWCNTs can improve the Young's modulus of thermoplastics by >300% [24]. However, only marginal improvement has been achieved in SWCNT-reinforced epoxies. There is a significant interest to greatly improve mechanical properties of epoxy-based matrices for aerospace and microelectronic applications.

Among the approaches mentioned above, surface functionalization of SWCNTs is advantageous because it can help address both the dispersion and adhesion needs. The functional groups on the SWCNT tube surfaces can improve the compatibility between SWCNTs and the surrounding matrix, thus minimizing aggregation of the nanotubes. The functional groups on the SWCNTs can also be used as precursors for the subsequent reaction to a wide variety of polymer matrices. Efforts on both noncovalent and covalent functionalization of SWCNTs have been reported [13]. Wrapping [25] and encapsulation

[26,27] are typical noncovalent functionalization approaches for SWCNTs. While the noncovalent functionalization does help improve dispersion significantly and maintain SWCNT physical properties, the lack of chemical bonding at the interface does not allow for effective load transfer. As a result, improvements in both modulus and strength of the polymer nanocomposite become limited.

On the other hand, covalent surface functionalization is more effective for load-bearing structural applications. The surface-functionalized SWCNTs can also potentially serve as cross-linkers to be integrated into the thermoset network [14,25]. It is noted that the functionalization of SWCNTs surfaces through extreme physical and chemical conditions [26,27] can result in defect formation on the tube surfaces, thus inevitably deteriorating the thermal, electrical and mechanical properties of SWCNTs. However, theoretical modeling has predicted that even a high degree of sidewall functionalization would degrade the mechanical strength of SWCNTs by only around 15% [28]. Considering the extremely high strength of SWCNTs, such a minor deterioration in mechanical strength should not affect the overall mechanical reinforcing effect of SWCNTs in polymer nanocomposites.

In most polymer/SWCNT nanocomposite research, it is desirable to prepare uniformly dispersed SWCNTs in a polymeric matrix to achieve overall high material performance and multi-functionality. However, a high concentration of SWCNT in the matrix would usually be needed to do so. This, in turn, would lead to a significant increase in cost and compromise in processability, especially for the fabrication of laminated composites by vacuum-assisted resin transfer molding (VaRTM). Alternative

approaches have to be undertaken to strategically place SWCNTs in locations of interest within the composite system.

In this thesis, 0.5 wt% of SWCNT in epoxy is utilized initially to investigate the maximum reinforcement effect of the SWCNT in epoxy without compromising processability. The SWCNTs are functionalized by oxidation, followed by grafting with polyamidoamine generation-0 (PAMAM-G0) dendrimers to chemically bridge between SWCNTs and epoxy. PAMAM-G0 dendrimers are monodispersed macromolecules having a regular, well-defined structure, which allows for the control of the number of functional group sites and size on the tube surfaces [29-31]. Because the amine groups on PAMAM-G0 can react with both the carboxylic acid groups on the oxidized SWCNT surfaces and epoxy monomers, it is expected that they can form a strong bonding between the matrix and SWCNTs. The effects of SWCNT dispersion and surface treatment on the mechanical properties of SWCNT reinforced epoxy composites are reported to understand their structure-property relationship.

Additionally, a new strategy for placing epoxy nanocomposites with high content of SWCNT at the location of interest by the preparation of partially cured (B-staged) epoxy/SWCNT thin films is reported. Because the films are partially cured, the SWCNT will be locked in place even after they are subsequently co-cured and integrated with neat epoxy. Since the thin films are prepared separately, higher SWCNT loadings can be incorporated in the polymer matrix without sacrificing processability, especially for the VaRTM process. Thus, desirable properties, such as good mechanical strength and high

electrical/thermal conductivities, can be achieved at a location of interest at much lower cost.

Specifically, the B-staged thin films are to be utilized as interleaves for enhancing conductivity and inter-laminar strength and toughness of the laminated VaRTM composites [32-37]. The increase in the inter-laminar strength and toughness can in turn improve compression after impact (CAI) strength of the composites [32,36]. Thus, thin films containing well dispersed SWCNTs, which usually exhibit improved modulus and toughness [11], appear to be an ideal candidate for reinforcement of laminated composites. In literature, a number of approaches have been developed to incorporate nanotubes into laminated composites which are shown to be effective [38]. However, those approaches require incorporation of nanotubes into the entire composite system [38] or by spraying of SWCNTs onto the substrate [39,40], which are not practical for large scale VaRTM productions. The proposed approach in this thesis to introduce a high concentration of SWCNTs into desired composite laminate locations is expected not only to help address the inter-laminar strength improvement needs but also to bring about SWCNT functionalities, such as high electrical and thermal conductivity, for aerospace composite applications.

In addition to the interleaf composite applications mentioned above, epoxy/SWCNT nanocomposite thin films may find a variety of other applications, such as micro-devices and electronic packaging [41-43] and coatings for corrosion protection [44]. If SWCNT alignment can be achieved during processing, significantly more applications can be expected [11].

## **THESIS LAYOUT**

As mentioned earlier, this work is mainly focused upon the preparation, processing and evaluation of mechanical and material properties of epoxy/SWCNT nanocomposite thin films. B-staged epoxy/SWCNT nanocomposite thin films at 50% of cure are the main focus of this research. Chapter II of this study focuses on the covalent oxidation and functionalization of SWCNTs. Chapter III focuses on the preparation of B-staged epoxy/SWCNT nanocomposite thin films. Chapter IV evaluates the morphology of epoxy/SWCNT based nanocomposites. Chapter V addresses the mechanical properties and fracture toughness of epoxy/SWCNT nanocomposites. With all of the background information determined at this stage, Chapter VI covers the effect sulfanilamide and nylon particles have on the overall system. Additional morphological, mechanical and material testing is performed. Results are explained in every chapter. Concluding remarks to summarize the findings of this research and recommendations for future related studies to be carried out are given in Chapter VII. The references and non-essential information follows in the last part of the thesis.

## **CHAPTER II**

### **COVALENT SURFACE OXIDATION AND FUNCTIONALIZATION OF SWCNTS: EFFECTS OF PAMAM-G0**

Chemically treating the surface of SWCNT is necessary in order to chemically bond the SWCNT to epoxy to impart their high mechanical properties to the overall nanocomposite. Oxidation of the SWCNT surface is used initially to form bonds with epoxy. Additionally, grafting the surface modifier PAMAM-G0 onto the oxidized surface is utilized to further improve its adhesion with epoxy. The effects of employing non-treated SWCNT to an epoxy/nanocomposite are described later.

#### **EXPERIMENTAL**

##### *Materials*

The epoxy resin and curing agent used in this study are EPIKOTE™ 862 resin (formerly Epon 862) and EPIKURE™ W curing agent (formerly Epicure W), both of which were obtained from Hexion Specialty Chemicals, Inc. The SWCNTs (XD Grade – 2/3 single wall carbon nanotubes, 1/3 ‘few wall’ carbon nanotubes and 5 wt% iron impurities) were provided by Carbon Nanotechnologies, Inc., with a reported density of ca. 1.35 g/cm<sup>3</sup>, and an aspect ratio of >1,000. The polyamidoamine (PAMAM) generation 0 (G0) dendrimer and sulfanilamide (99%) were purchased from Sigma-Aldrich. The nylon particles (Nylon 12) with particle size around 10 μm and a melting point around 165 °C was donated by Toray Industries Inc. Concentrated sulfuric

acid (95.4%) and nitric acid (70%) were obtained from Fisher Scientific. Polyvinylidene difluoride (PVDF) filter membranes with a pore size of 45  $\mu\text{m}$  were purchased from Millipore. All chemicals were used as received.

### *Preparation*

A sample of 1.0 g of SWCNTs was first oxidized by a mixture of 180 mL of concentrated sulfuric acid and 60 mL of concentrated nitric acid in a round-bottom flask. The mixture was ultrasonicated in an ultrasonication bath for 2.5 hours. After sonication, 760 mL of de-ionized water was added to the sample and the system was sonicated for three more hours. Oxidized SWCNTs (O-SWCNTs) were obtained at this step. The O-SWCNT sample was then collected through a PVDF filter membrane and washed several times with de-ionized water to remove acid residues. The cleaned O-SWCNTs were then re-dispersed in 500 mL acetone by an additional three hours of sonication. The O-SWCNTs were further treated by interacting with PAMAM-G0 dendrimer.

### *X-Ray Photoelectron Spectroscopy*

X-ray photoelectron spectroscopy (XPS) is a quantitative spectroscopic technique that measures the elemental composition, empirical formula, chemical state and electronic state of the elements that exist within a material. The XPS spectra of oxidized SWCNTs were obtained using a Kratos Axis Ultra multitechnique spectrometer. Non-monochromatic Mg  $K_{\alpha}$  photons were used for all the measurements. The atomic composition of the sample surfaces was calculated using the high resolution

peak areas for the main core XPS line of each element in conjunction with the empirical sensitivity factors provided by the instrument manufacturer and the application of a Shirley-type background correction. The binding energy of the C(1s) was set at 284.5 eV as the reference for all other peaks [38].

## **RESULTS AND DISCUSSION**

The oxidation of SWCNT by strong acids has been reported [34,35]. When using a mixture of concentrated sulfuric acid and nitric acid, the SWCNT surfaces will form carboxylic acid groups [34,39]. The presence of carboxylic acid functionalities on the tube surfaces offers possibilities for subsequent tailored SWCNT surface functionalization. Also, the oxidation process can effectively cut the SWCNT ropes into shorter tubes [34]. This helps to not only unwrap the tube bundles but also improve dispersion of SWCNTs in organic solvents.

The XPS characterization shows that oxidation of SWCNTs surfaces has taken place and allows for estimation of the degree of oxidation on the tube surfaces. The XPS spectrum of oxidized SWCNT C(1s) peak in Figure 1 shows a shoulder at a higher binding energy region. This shoulder is resulted from the carboxylic acid groups on the tube surfaces[38].

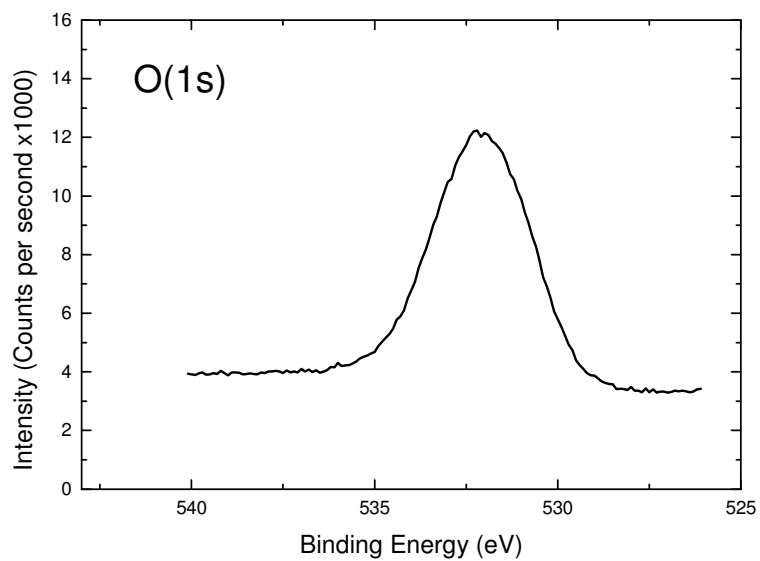
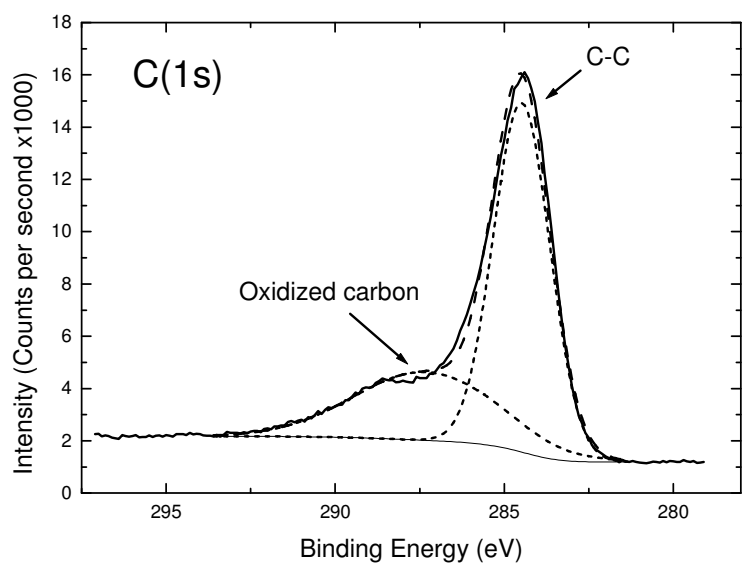


Figure 1 XPS spectra of oxidized SWCNT (O-SWCNT)

The existence of the O(1s) peak provides additional evidence of SWCNT oxidation. By quantifying the ratio of C and O on oxidized SWCNT surfaces, it is estimated that the atomic ratio of C and O is about 4:1. Considering that each carboxylic acid group contains two oxygen atoms, it is estimated that 1/8 of the carbon atoms on SWCNTs has been oxidized to form carboxylic acid groups. Thus, the theoretical stoichiometric ratio between SWCNT and PAMAM-G0 is 64:1 since each PAMAM-G0 molecule contains eight amine groups (four primary amine and four secondary amine groups). In order to allow for the amine groups in PAMAM-G0 to be co-cured with epoxy monomers, theoretically the amount of PAMAM-G0 utilized should be higher than the stoichiometric ratio so that the functionalized SWCNTs can be chemically bonded to epoxy in Figure 2.

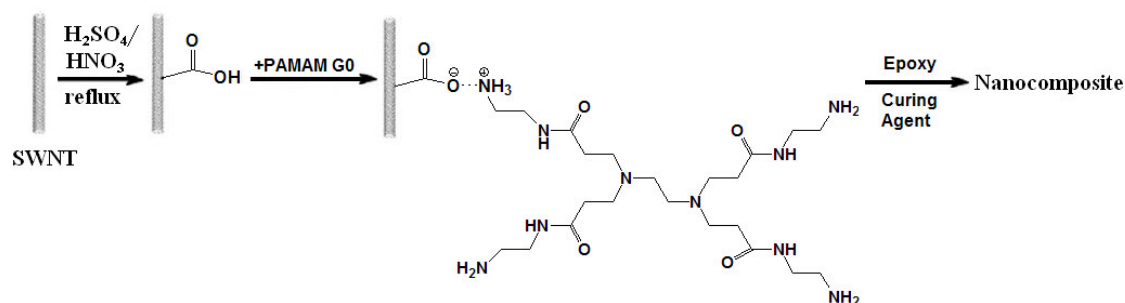


Figure 2 Schematic of functionalization of SWCNT by PAMAM-G0

PAMAM-G0 molecule introduced extra amine groups to the SWCNTs. The extra amine groups can be co-cured with the epoxy monomer to integrate SWCNT into the epoxy network. However, it is believed that free amine functional groups in

PAMAM-G0 will be present even at the theoretical stoichiometric ratio because of the steric hindrance effect on the PAMAM-G0 molecules. Consequently, excess amine groups on the SWCNT surfaces will likely react with epoxy and form a chemically bonded network structure. In this research, a formulation of SWCNT:PAMAM-G0 = 64:1 (molar ratio) was adopted to prepare epoxy/F-SWCNT. Details about the interaction between O-SWCNT and the PAMAM-G0 dendrimer to form PAMAM-G0 functionalized SWCNTs (F-SWCNTs) can be found elsewhere [45].

## **CHAPTER III**

### **PREPARATION OF B-STAGED EPOXY/SWCNT NANOCOMPOSITE THIN FILMS FOR VARTM APPLICATIONS**

The procedure for preparing B-staged epoxy/SWCNT nanocomposite thin films is described. Numerous difficulties had to be overcome to prepare good quality epoxy/SWCNT thin films. With the addition of SWCNT to epoxy, there is a significant increase in viscosity of the sample. How well the B-stage thin films are prepared depends strongly on the control of the nanocomposite viscosity. If the viscosity of the B-staged sample is too high, significant film defects on the surface will form. If the viscosity is too low, voids will appear in the thin film after film formation. Evaluation of all aspects of the film process is described.

#### **EXPERIMENTAL**

##### *Materials*

The thin film coater was purchased from Elcometer Inc. (Rochester Hills, Michigan) where a temperature control system was later added in our lab. The release paper was donated by Hexcel Corporation (Salt Lake City, UT). All chemicals were used as received.

### *Thin Film Preparation*

The F-SWCNTs, which were well dispersed in acetone, were then added to the epoxy monomer at a predetermined ratio and sonicated for 15 min. to achieve a final SWCNT loading of 0.5 wt% in the final nanocomposite. Multiple samples were prepared in conjunction with the multiple states of SWCNT treatment. The three states of SWCNT used were pristine SWCNT (P-SWCNT), oxidized SWCNT (O-SWCNT) and functionalized SWCNT (F-SWCNT). After removal of acetone with a rotavapor (rotary evaporator) in a water bath at 70°C, the curing agent was added (26.4 parts by weight per 100 parts by weight of EPIKOTE<sup>TM</sup> 862). The epoxy/SWCNT mixture was further degassed to remove the remaining air bubbles trapped within the sample.

The samples were then B-stage cured at 121°C for 70 minutes in an oven. Prior to removal of the epoxy/SWCNT samples from the oven, the thin film coater was preheated to 90°C. The epoxy/SWCNT samples were quickly transferred from the oven and immediately cast into thin films at a thickness of 50 µm on release paper which was laid on the thin film coater. For comparison purposes, B-stage cured neat epoxy thin films were also prepared following the same procedures.

Bulk epoxy/nanocomposite samples were also prepared in order to obtain its mechanical behavior. The resin mixture was degassed and cast in a preheated glass mold and cured in an oven at 121 °C for 2 hrs, followed by 2 hrs of post-cure at 177 °C.

### *Differential Scanning Calorimetry*

Differential Scanning Calorimetry (DSC) is a thermoanalytical technique in which the difference in the amount of heat required to increase the temperature of a sample and reference are measured as a function of temperature. A Mettler Toledo (Model DSC821<sup>e</sup>) differential scanning calorimeter was used to obtain DSC thermograms. The samples were kept isothermal at 121 °C for 70 min to mimic the B-stage curing process in the oven; and kept isothermal at 177 °C for two hours to mimic the complete curing condition. The experiments were carried out under a nitrogen gas purge (80 mL/min).

## **RESULTS AND DISCUSSION**

The film preparation is successful in achieving visually defect-free B-staged thin films. This effective approach involves B-stage curing the epoxy samples in an oven, followed by the formation of the B-stage thin films using a commercial film coater. In this research, after B-staged cure, the sample still possesses sufficient fluidity for thin film casting meanwhile being able to maintain relatively high viscosity to avoid void formation. Maintaining the thin film coater at an appropriate temperature (90 °C in this case) is also critical for the film casting to prevent the epoxy/SWCNT nanocomposite from excessive hardening, thus preserving the formability of the films during the film casting process. More detailed information on viscosity is described later.

In this study, 50% degree of cure for epoxy samples appears to be ideal for handling, insertion, and integration of the thin films for VARTM composite

reinforcement. However, for other material systems and applications, other sets of processing parameters may need to be utilized to prepare good quality thin films for intended applications. The degree of cure is desired to achieve around 50% of epoxy curing in the final thin films to allow for the B-stage cured samples to co-cure with the newly injected epoxy monomers and curing agent. In the meantime, at 50% level of curing, the well dispersed SWCNTs in the epoxy thin film remain locked in place in the inter-laminar region to help strengthen the inter-laminar strength and thermal/electrical conductivity.

The curing processes of the epoxy samples were monitored by DSC. The degree of cure was estimated by the ratio of the exotherm during the B-staged curing ( $\Delta H_B$ ) to the exotherm during a complete cure ( $\Delta H_C$ ) of the same sample, as shown in Figure 3. The DSC results show that the epoxy is almost 100% cured at 177 °C for 90 minutes, but requires a much longer curing time at 121 °C. For the epoxy nanocomposite systems investigated here, it is determined that 70 minutes at 121 °C yields approximately 50% cure of the samples as shown in Table 1.

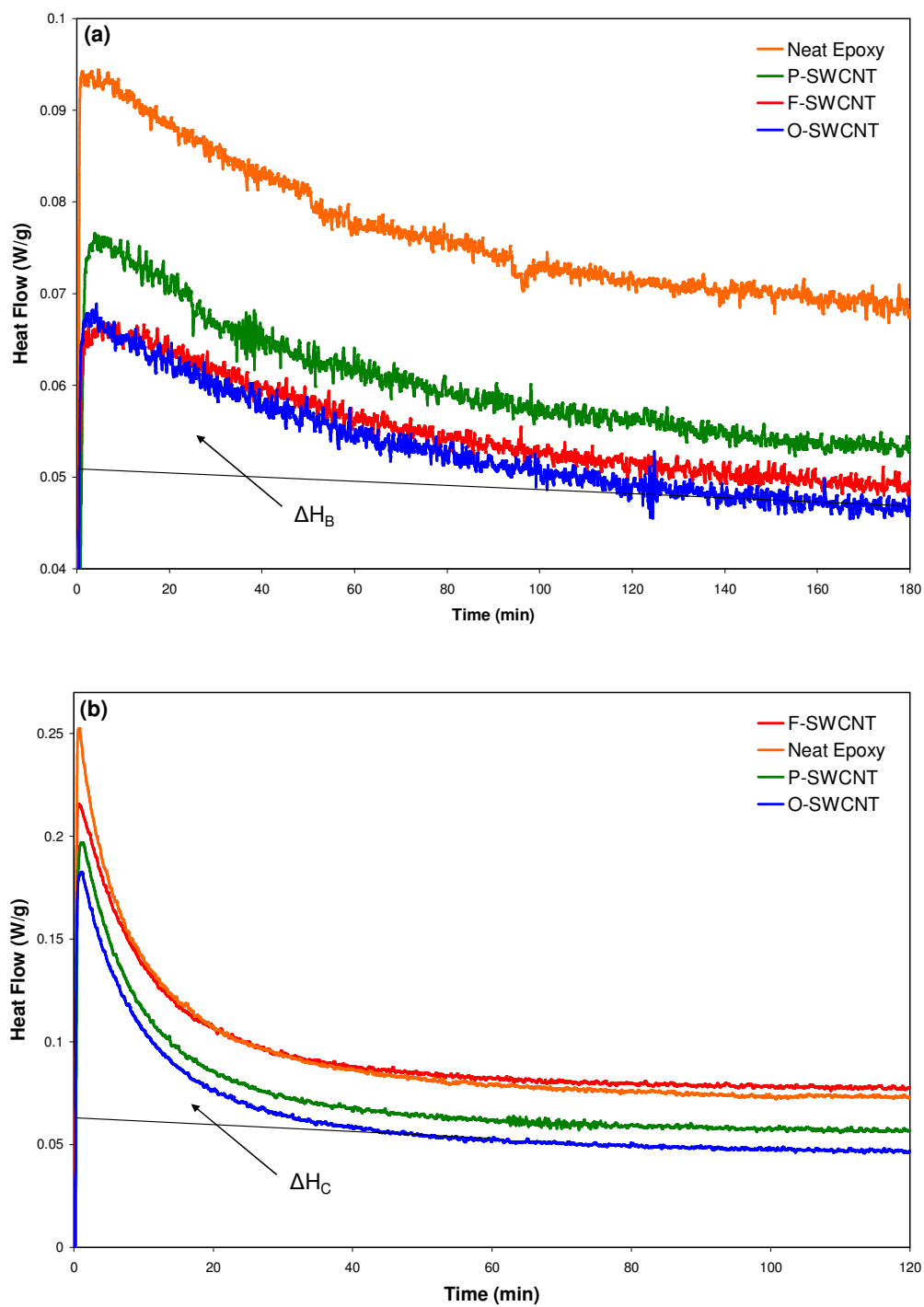


Figure 3 DSC thermograms of epoxy/SWCNT nanocomposite thin films.

(a) samples cured at 121°C for 3 hours, (b) samples cured at 177°C for 2 hours

Table 1 Required time to achieve a 50% B-stage cured thin film at 50  $\mu\text{m}$  thickness

Sample (0.5 wt%)	Curing Temperature	Curing Time	Degree of Cure
Neat Epoxy	121 °C	70 min	50.1%
Epoxy/P-SWCNT	121 °C	60 min	31.1%
Epoxy/O-SWCNT	121 °C	75 min	67.4%
Epoxy/F-SWCNT	121 °C	65 min	41.1%
Epoxy/F-SWCNT	121 °C	70 min	50.9%

#### *Thin Film Temperature Properties*

Both the B-stage cured thin film samples and fully cured thin film samples have been characterized by DSC, as shown in Figure 4. The DSC thermograms in part a of the figure on page 20 show that the B-stage cured epoxy/SWCNT thin films have a melt range of around 50-57 °C. Such a melt range assures that the B-staged thin films remain stable at room temperature. Meanwhile, they can be easily processed upon heating. Such a property facilitates their subsequent VARTM processing.

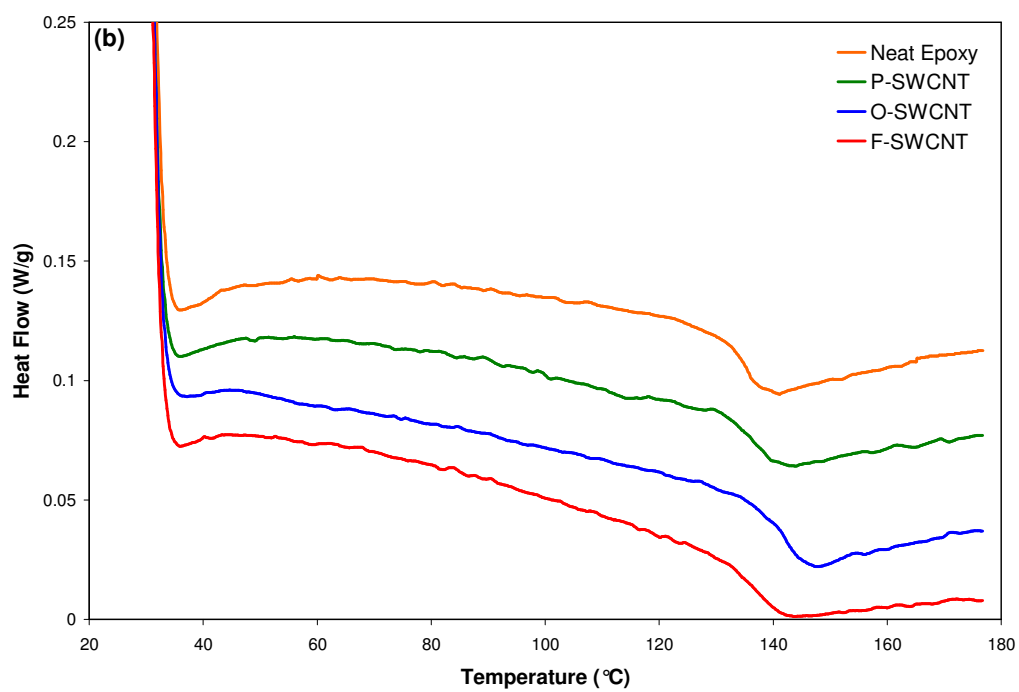
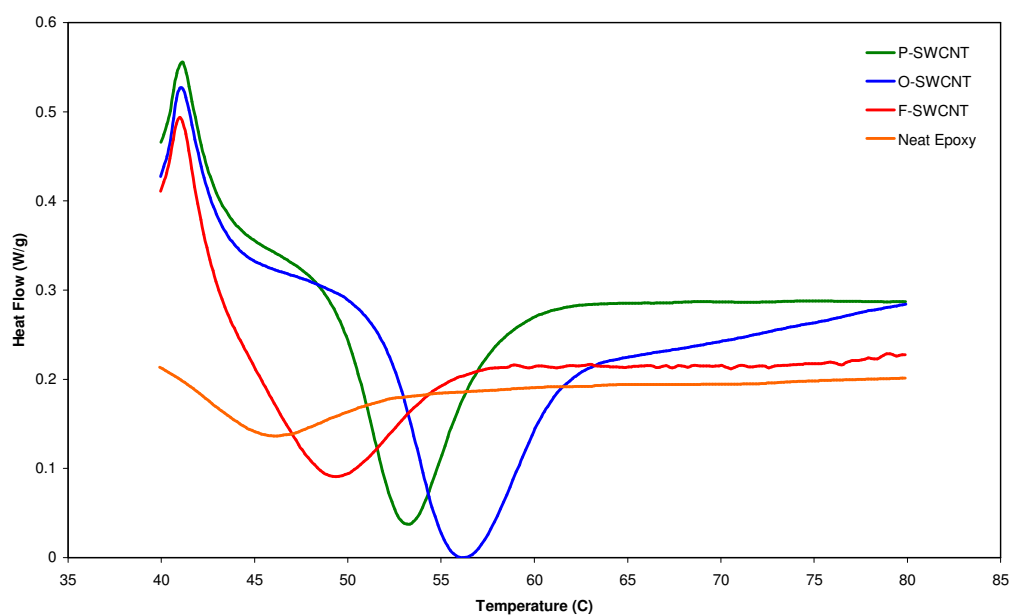


Figure 4 DSC thermograms of (a) 50% cured thin films, (b) 100% cured thin films

The DSC characterization of the fully cured thin films in part b of the figure on page 20 shows that there is a minor variation in  $T_g$  from 136 to 144 °C among the four film samples. Such a small variation has been observed earlier and is believed to be due to: 1) the trapping of the curing agent around the SWCNT bundles, 2) the side reactions of the curing agent with O-SWCNTs or 3) the side reactions of the curing agent with the PAMAM-G0 dendrimers. All of the above possibilities lead to the alteration of the curing stoichiometric ratio and thus minor variation in  $T_g$  [45].

The incorporation of 0.5 wt% SWCNTs in epoxy is found to have little effect on the overall curing process. The above methodology is shown to give rise to good quality B-staged thin films. The epoxy thin films containing P-SWCNT, O-SWCNT, and F-SWCNT exhibit similar visual appearance. All the film samples can be easily handled and placed in the inter-laminar regions of the laminated composites for VARTM processing.

## **CHAPTER IV**

### **MORPHOLOGY OF EPOXY/SWCNT BASED NANOCOMPOSITES**

Numerous testing methods are utilized in this chapter to more closely evaluate the epoxy/SWCNT nanocomposites dispersion and adhesion with the epoxy matrix. The differences between the different treatment methods are clearly visible which allows for determinations to be made about the improvement upon the adhesion and dispersion of SWCNTs in epoxy/nanocomposites.

#### **EXPERIMENTAL**

##### *Scanning Electron Microscopy*

A scanning electron microscope (SEM) is a type of electron microscope that images a sample's surface by scanning it with a high-energy beam of electrons in a raster scan pattern. SEM images of the fracture surfaces of the nanocomposites were acquired using a Zeiss Leo 1530 VP Field Emission-SEM (FE-SEM). The samples were quenched in liquid nitrogen and then broken to obtain fresh fracture surfaces. The fracture surface was sputter-coated with a thin layer (ca. 3 nm) of Pt/Pd (80/20) prior to SEM imaging. SEM images were also acquired using a JEOL-6400 SEM. The acceleration voltage was kept at 15 kilovolts. The fracture surface was sputter-coated with a thin layer (ca. 3 nm) of Au/Pd prior to SEM imaging.

### *Transmission Electron Microscopy*

Transmission electron microscopy (TEM) is a microscopy technique whereby a beam of electrons is transmitted through an ultra thin specimen, interacting with the specimen as they pass through. TEM and high-resolution transmission electron microscopy (HR-TEM) images of nanocomposites were obtained by using a JEOL 2010 high-resolution transmission electron microscope operated at 200 kV. A Reichert-Jung Ultracut-E microtome was utilized to prepare thin sections of nanocomposites with thickness of 70-100 nm for TEM and HR-TEM imaging.

### *Raman and Optical Microscopy*

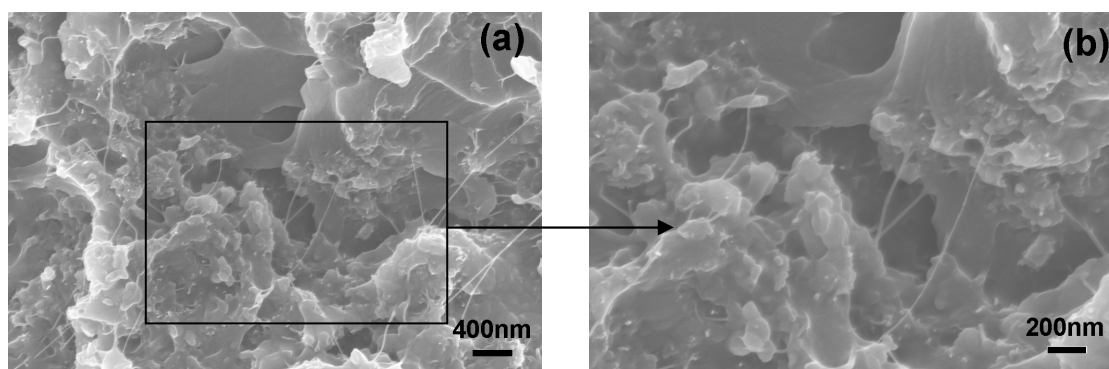
Raman and optical microscopy were employed to assess and visualize the dispersion and distribution of SWCNTs in the epoxy matrix. The Raman microscope consists of a T64000 Horiba JY triple spectrometer coupled to a confocal optical microscope furnished with an XYZ motorized stage. A microscope objective ( $\times 50$ ) was used to focus the 632.8 nm laser beam to a focal cylinder of ca. 1.5  $\mu\text{m}$  in diameter and ca. 7  $\mu\text{m}$  in height, the latter given by the depth of focus. The confocal layout of the microscope ensured that only light scattered within the confocal cylinder was directed to the spectrometer. The focused laser beam was raster scanned on the sample surface and a Raman spectrum excited at each step of the scan was recorded for parallel incident and scattered light polarizations. The collected data formed a hyperspectral cube of the scanned area, which contained both spectral and spatial information.

## RESULTS AND DISCUSSION

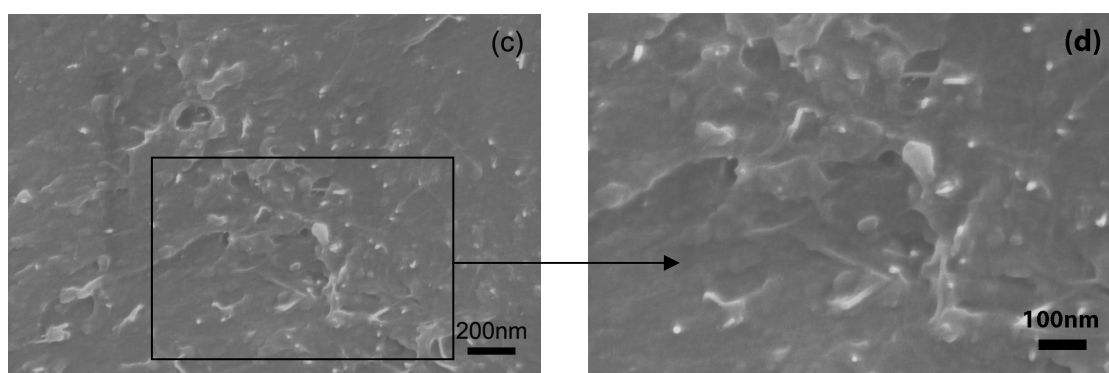
### *Dispersion*

Achieving a high degree of dispersion of SWCNTs in epoxy is crucial for producing nanocomposites with desirable properties. Typical SWCNT aggregates are micrometers in size. Their dispersion is also generally poor. These imperfections can significantly compromise the nanocomposite properties, especially the mechanical properties. A high degree of dispersion of SWCNTs in thin film interleaves is needed for achieving high CAI strength in composites [36].

It was observed that the viscosity of neat epoxy increased significantly after the addition of F-SWCNT. This indicates that F-SWCNTs have been well dispersed in epoxy monomer [14]. SEM investigation on freeze-fractured epoxy/SWCNT nanocomposites surfaces can clearly show the state of dispersion of SWCNTs in epoxy in Figure 5. The SEM image of the epoxy/P-SWCNT sample (Figure 5a) shows that the P-SWCNTs are agglomerated and the adhesion between P-SWCNT and epoxy is generally poor, as many P-SWCNTs are pulled out of the matrix and show no sign of epoxy matrix attached to the bare P-SWCNT bundles. While on the fracture surface of the epoxy/F-SWCNT sample (Figure 5b), it is shown that the SWCNTs are not only well dispersed throughout the matrix but their adhesion to the epoxy matrix is also greatly improved since most of the F-SWCNTs on the fracture surface are broken.



(a) Epoxy/P-SWCNT: poor dispersion, poor adhesion (b) Epoxy/F-SWCNT: enlarged region from (a)



(c) Epoxy/F-SWCNT: good dispersion, good adhesion (d) Epoxy/F-SWCNT: enlarged region from (c)

Figure 5 SEM images of fracture surface of nanocomposite samples

Based on the above findings, the PAMAM-G0 functionalization and co-curing with epoxy monomers can improve both the dispersion and adhesion between F-SWCNTs and epoxy matrix. The morphology of epoxy/F-SWCNT is further investigated by TEM and HR-TEM. As shown in Figure 6a, F-SWCNTs appear to be unevenly dispersed.

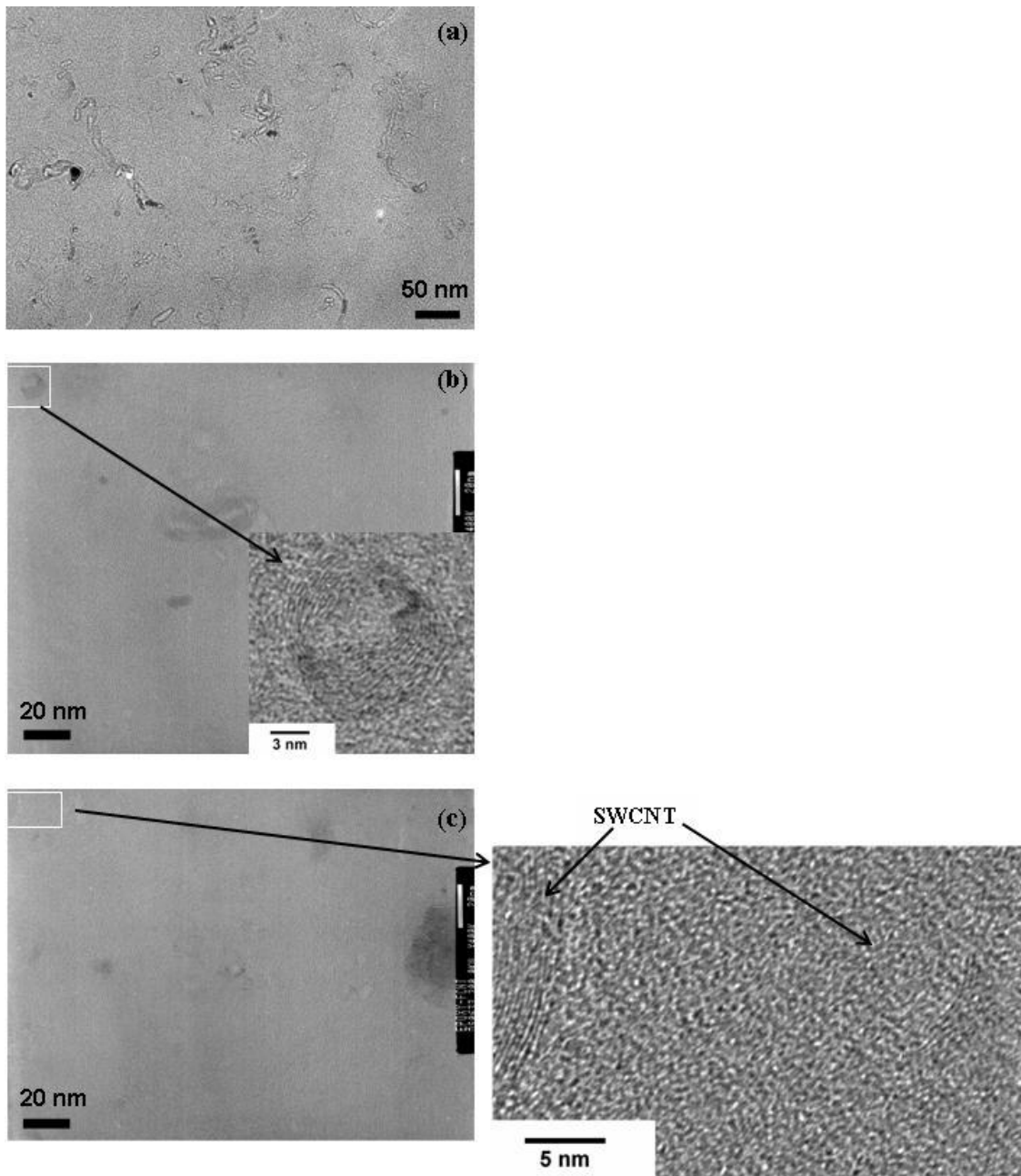


Figure 6 TEM image of epoxy/F-SWCNT. (a): a representative region with visible SWCNTs. (b) and (c): magnified regions which are almost featureless on low magnification images

Some regions appear to be free of F-SWCNTs. By focusing on the seemingly SWCNT-free regions, as shown in Figures 6b and 6c, individually dispersed or bundles of F-SWCNTs are found to be well dispersed in epoxy. In the inset of Figure 6b, a small bundle of F-SWCNTs can be observed. The HR-TEM image of a randomly selected region in Figure 6c shows individual F-SWCNTs. The above results suggest that the F-SWCNTs were still not completely exfoliated even after oxidation and surface functionalization. The F-SWCNTs shown in Figure 6a, and the shaded regions in Figures 6b and 6c are actually bundled or aggregated F-SWCNTs. However, some of the F-SWCNTs have been completely exfoliated into individual tubes. It should be noted that none of the F-SWCNTs observed is straight. They have all curled up. Curled SWCNTs are ineffective in improving epoxy modulus.

The oxidation of SWCNTs and the reaction with PAMAM-G0 dendrimer has been shown to be an effective approach to functionalize SWCNTs, especially for the preparation of epoxy based nanocomposites [45]. The dispersion and distribution of SWCNTs in polymer matrix have been mainly characterized by scanning electron microscopy and transmission electron microscopy [11-13,45]. In this research, the morphology of epoxy/SWCNT thin films was characterized by Raman and optical microscopy as well. The Raman spectrum of SWCNT has a strong Raman band at  $1580\text{--}1590\text{ cm}^{-1}$ , called the G-band [46], which corresponds to predominantly stretching C–C vibrations with eigenvectors tangential to the nanotube surface. On the other hand, the epoxy matrix in the samples gives structureless Raman responses having mostly a fluorescence origin. This makes Raman microscopy an ideal tool to characterize the

dispersion of epoxy/SWCNT nanocomposites. Two types of Raman images produced from the hyperspectral cube are presented. One way to visualize the carbon nanotubes dispersion is to plot the G-band Raman intensity distribution over the scanned area. In the other approach, reference Raman spectra of SWCNT and the epoxy matrix are used to deconvolute the spectra contained in the hyperspectral cube to two components and present their distribution in a single Raman image. The first type of Raman imaging displays better regions with high concentration of nanotubes in the sample, whereas the second one depicts improvements over those containing small amounts of SWCNT.

The spatial resolution of the Raman images is determined by the size of the focused laser beam which is diffraction limited. However, the Raman images recorded at sampling steps smaller than the laser spot size have higher contrast than those obtained at the native resolution. A comprehensive description of the Raman imaging of SWCNT can be found elsewhere [47].

Figure 7(a) presents the optical image of a  $80 \times 80 \mu\text{m}^2$  scanned area on the surface of an epoxy/P-SWCNT (0.5 wt%) nanocomposite thin film sample. The reference Raman spectra of the carbon nanotubes and epoxy matrix used for deconvolution of the hyperspectral cube are displayed in Figure 7(b). The Raman image showing the nanotubes (orange color) and epoxy (green color) distribution is given in Figure 8(c) and the G-mode intensity distribution is shown in Figure 7(d). Figures 8 and 9 display the Raman images of epoxy/O-SWCNT (0.5 wt%) and epoxy/F-SWCNT (0.5 wt%) nanocomposites, respectively, collected at the same conditions as the ones shown in Figure 7.

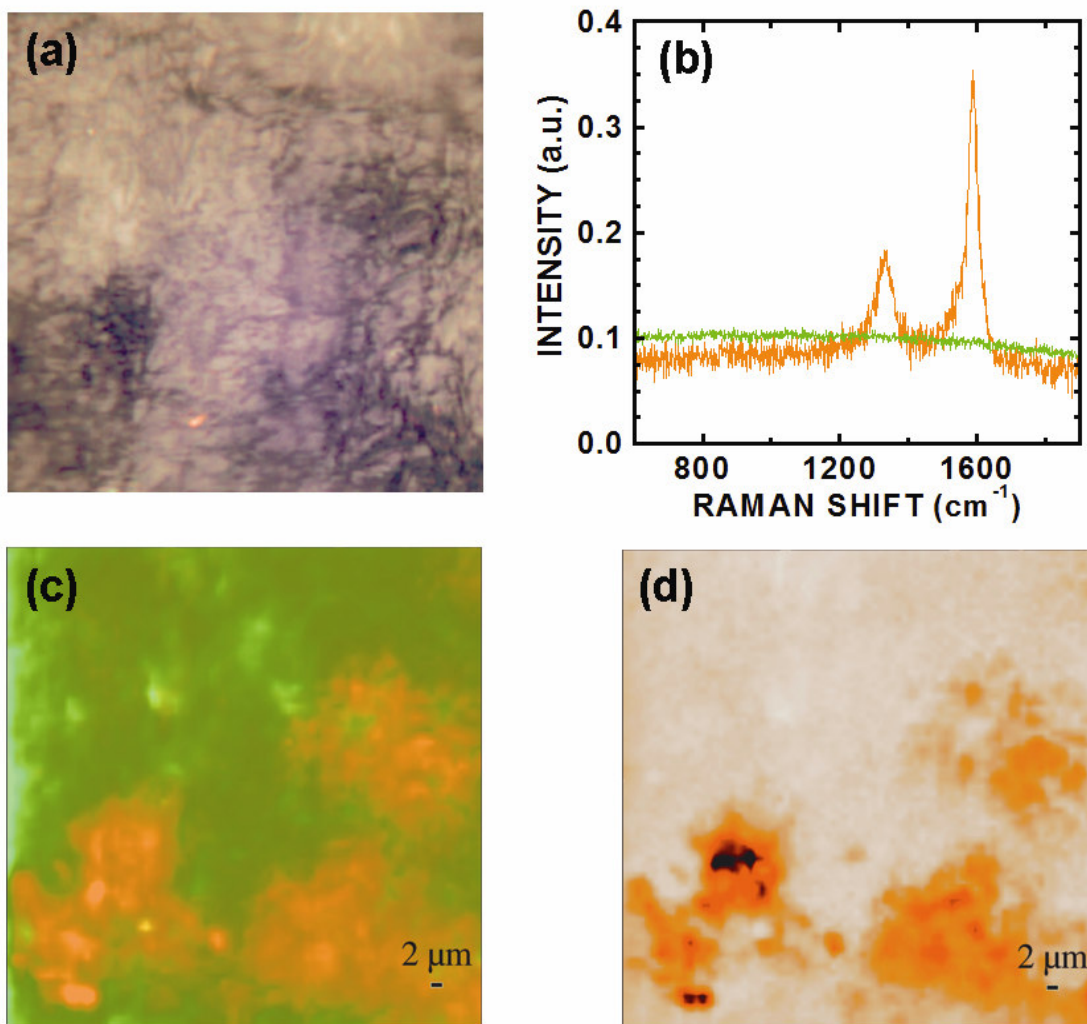


Figure 7 Optical image of  $80 \times 80 \mu\text{m}^2$  area on the surface of an epoxy/P-SWCNT (0.5 wt%) nanocomposite thin film. (a); reference Raman spectra of P-SWCNT (orange color) and epoxy matrix (green color) (b) used for producing the Raman image in (c), brighter colors denote higher intensity; G-band intensity distribution, darker color corresponds to higher intensity (d)

The Raman images shown in Figures 7 to 8 demonstrate a gradual improvement of SWCNTs dispersion in going from P-SWCNTs to O-SWCNTs. The epoxy/P-SWCNT nanocomposite thin film exhibits the lowest degree of dispersion among the tested samples. The SWCNTs are aggregated at 10 to 50  $\mu\text{m}$  size, and substantial regions of the nanocomposite are free of SWCNTs. The SWCNT distribution within the agglomerates is highly inhomogeneous and the SWCNTs are differently strained. Given the dependence of the G-band position on nanotubes strain [48,49], it can be estimated that the difference in strain between the outer carbon nanotubes in an agglomerate and those in the core is ca. 0.4%.

Oxidation of the SWCNT apparently helps to improve their dispersion in the epoxy matrix as shown in Figure 8. The distribution remains uneven but O-SWCNTs are dispersed practically in the entire volume of the nanocomposite thin film leaving only small pockets of pure epoxy material.

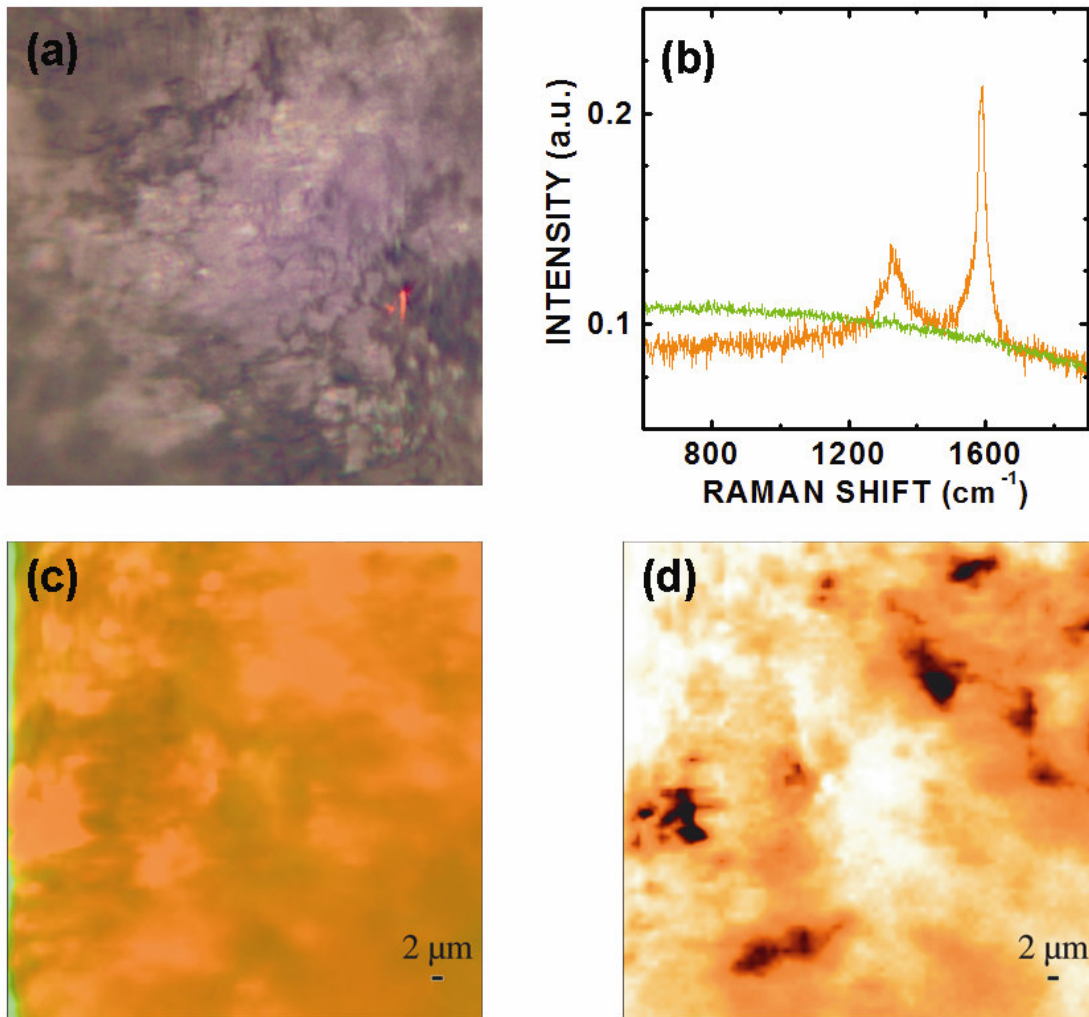


Figure 8 Optical image of  $80 \times 80 \mu\text{m}^2$  area on the surface of an epoxy/O-SWCNT (0.5 wt%) nanocomposite thin film. (a); reference Raman spectra of O-SWCNT (orange color) and epoxy matrix (green color) (b) used for producing the Raman image in (c), brighter colors denote higher intensity; G-band intensity distribution, darker color corresponds to higher intensity (d)

The epoxy/F-SWCNT nanocomposite thin film exhibits the best dispersion among the three samples. The Raman images in Figure 9 demonstrate remarkably smooth distribution of the F-SWCNT in the nanocomposite with some concentration irregularities seen in Figure 9(d) of size below 1  $\mu\text{m}$ . The results presented in Figure 9 show that PAMAM-GO functionalized SWCNT leads to a high degree of SWCNT dispersion at micron length scale nanocomposites with far better quality than those produced using pristine or oxidized SWCNTs. It should be noted that the above findings are consistent with an earlier work on an investigation of SWCNT dispersion due to surface functionalization using scanning electron microscopy and transmission electron microscopy [45].

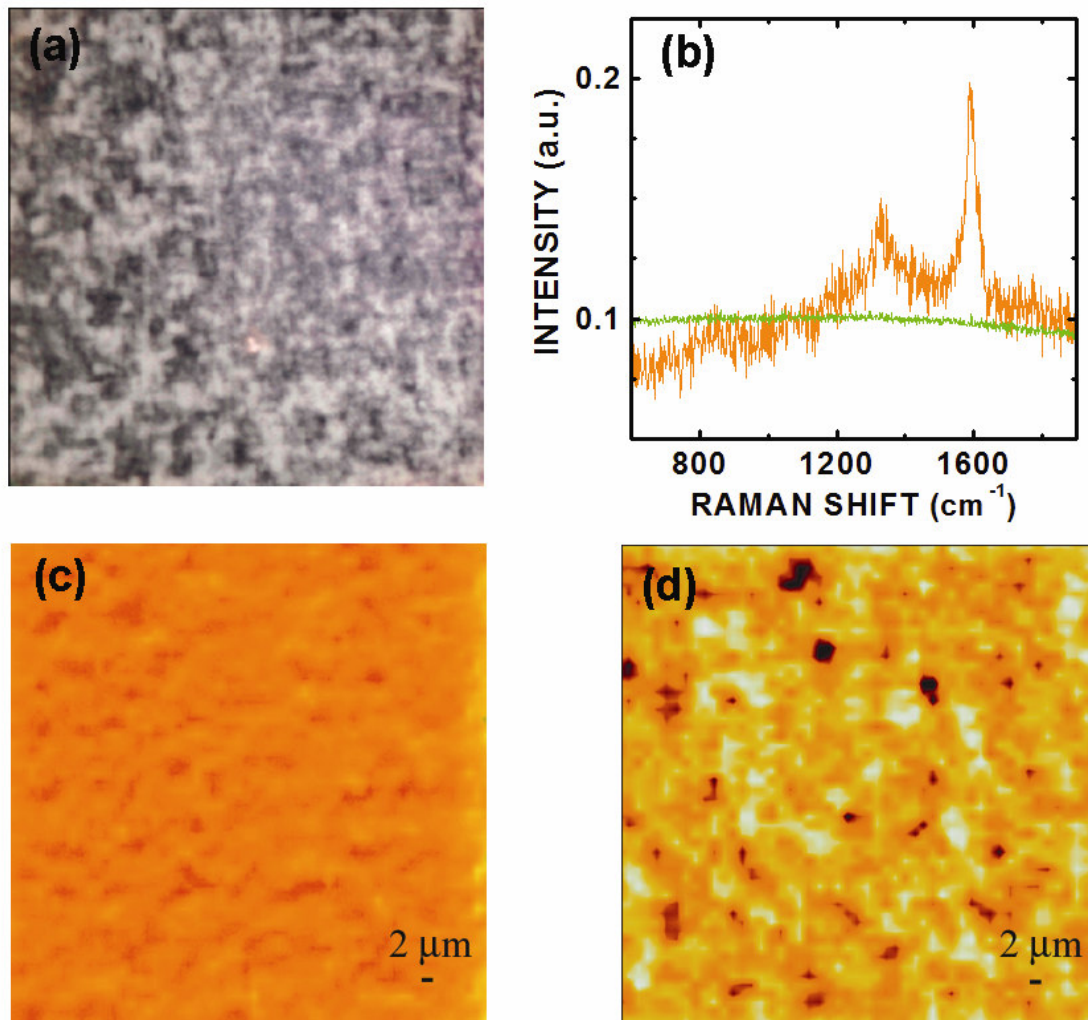


Figure 9 Optical image of  $80 \times 80 \mu\text{m}^2$  area on the surface of an epoxy/F-SWCNT (0.5 wt%) nanocomposite thin film. (a); reference Raman spectra of F-SWCNT (orange color) and epoxy matrix (green color) (b) used for producing the Raman image in (c), brighter colors denote higher intensity; G-band intensity distribution, darker color corresponds to higher intensity (d)

## **CHAPTER V**

### **MECHANICAL PROPERTIES AND FRACTURE TOUGHNESS OF EPOXY/SWCNT BASED NANOCOMPOSITES**

Numerous mechanical and material properties were determined to give further insight into the behavior of epoxy/SWCNT nanocomposites. The mechanical property and fracture toughness information is very important in terms of the viability of epoxy/SWCNT systems.

#### **EXPERIMENTAL**

##### *Tensile Testing*

Tensile properties of epoxy nanocomposites were obtained based on ASTM D638-98 method. The tensile tests were performed using an MTS<sup>®</sup> servo-hydraulic test machine at a crosshead speed of 5.08 mm/min at ambient temperature. Young's modulus, tensile strength and elongation at break of each sample were obtained based on at least five specimens per sample. The average values and standard deviations were reported.

##### *Dynamic Mechanical Testing*

Dynamic mechanical analysis (DMA) is useful for studying the viscoelastic nature of polymers. DMA was conducted using a Q800 dynamic mechanical analyzer (TA Instruments) under three-point-bending mode, ranging from room temperature to 200.0 °C, at a fixed frequency of 1 Hz and with a temperature increment of 3.00 °C/min.

The maximum point on the  $\tan \delta$  curve was chosen as the glass transition temperature ( $T_g$ ) of the sample.

### *Fracture Toughness*

Fracture toughness is a property which describes the ability of a material containing a crack to resist fracture. Fracture toughness tests were conducted based on the linear elastic fracture mechanics (LEFM) approach. The single-edge-notch 3-point-bending (SEN-3PB) test, based on ASTM D5045, was performed to obtain the mode-I critical stress intensity factor ( $K_{IC}$ ) of the neat epoxy and epoxy nanocomposites reinforced with SWNTs. At least five specimens per sample were tested to determine  $K_{IC}$  values of the samples. The critical stress intensity factors were calculated using the following equation:

$$K_{IC} = \left[ \frac{P \times S}{B \times W^{3/2}} \right] \times f(a/W)$$

where  $P$  is the load at crack initiation,  $S$  is the span width,  $B$  is the thickness of the specimen,  $W$  is the width of the specimen,  $a$  is the initial crack length, and  $f(a/W)$  is the geometry correction factor.

## RESULTS AND DISCUSSION

### *Mechanical Properties*

Tensile testing was performed to evaluate the effect of the SWCNT treatment on the mechanical properties of the epoxy nanocomposites. The key tensile properties are listed in Table 2 and tensile stress versus strain curves for all samples are shown in Figure 10.

Table 2 Mechanical properties of bulk epoxy/SWCNT nanocomposites (0.5 wt%)

Property	Neat Epoxy	Epoxy/P-SWCNT	Epoxy/O-SWCNT	Epoxy/F-SWCNT
Young's Modulus (GPa)	2.77±0.01	2.84±0.05	3.17±0.01	3.21±0.15
Tensile Strength (MPa)	60.1±5.6	74.2±0.5	76.5±3.9	82.7±3.2
Elongation (%)	1.98±0.22	2.57±0.18	2.97±0.40	4.88±0.91
K <sub>IC</sub> (MPa•m <sup>1/2</sup> )	0.78±0.01	0.76±0.03	0.83±0.05	0.93±0.04

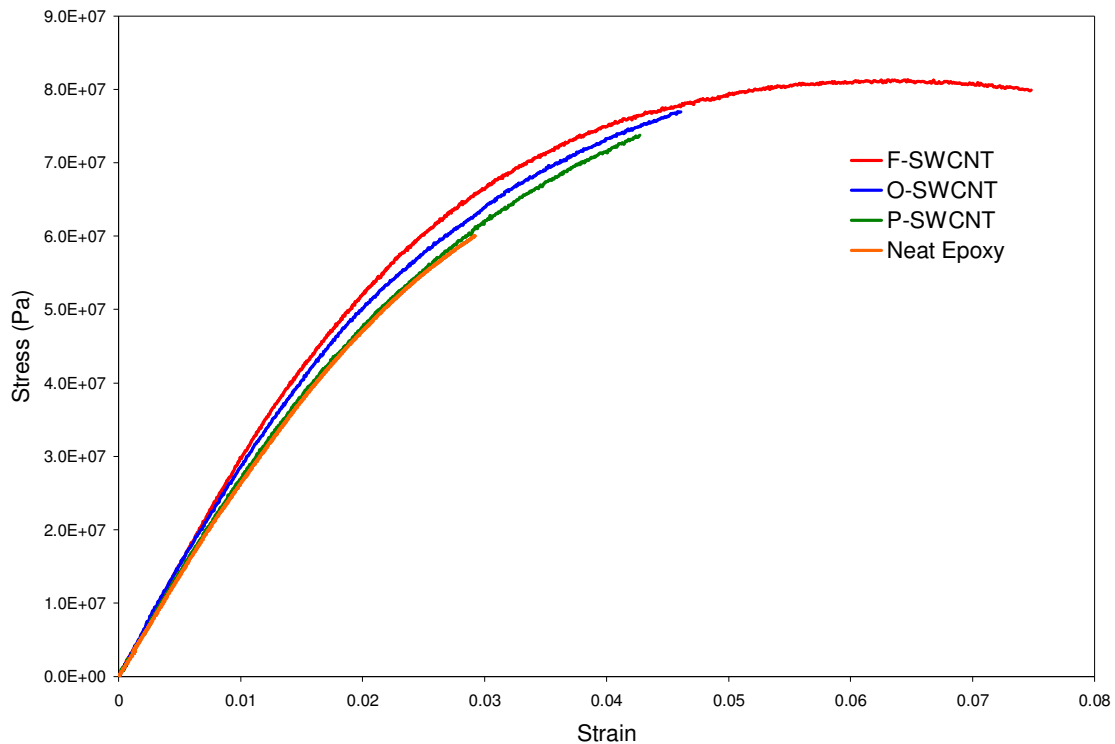


Figure 10 Tensile curves of epoxy/SWCNT nanocomposites

The results show that the incorporation of P-SWCNT can improve the epoxy Young's modulus and tensile strength by 3% and 23%, respectively. The limited improvement on tensile properties is believed to be due to the poor SWCNT dispersion in epoxy matrix, as evidenced in Figure 8. Oxidation of SWCNTs leads to a much better dispersion effect and thus the mechanical properties of epoxy/O-SWCNT were further improved. The incorporation of F-SWCNTs leads to the best overall reinforcement effect in modulus and strength by 16% and 35%, respectively. The tensile properties of the nanocomposite samples show a good correlation with the level of dispersion of SWCNTs in the epoxy matrix. The above study suggests that, as expected, the better the dispersion

of SWCNT in epoxy results in better improvements in mechanical properties. The much higher elongation at break for the epoxy/F-SWCNT nanocomposite compared to neat epoxy signifies that the sizes of SWCNT domain are smaller than the critical flaw size for epoxy. Furthermore, the addition of PAMAM-G0 as a surface modifier for SWCNT might alter epoxy curing and matrix properties. It is worthwhile to mention that the data above are the bulk properties of the nanocomposites. If SWCNTs can be better aligned in the thin film samples, the thin films will exhibit an even better improvement on mechanical properties along the SWCNT orientation.

The  $K_{IC}$  of the samples are listed in Table 2. There is no noticeable difference in  $K_{IC}$  values among the neat epoxy and epoxy/P-SWCNT, which is probably because the epoxy resin is inherently brittle and SWCNTs themselves cannot promote effective toughening mechanisms, such as shear banding and crack bridging, in epoxy. The observed fracture toughness improvement in epoxy/F-SWCNT is believed to be not from the presence of F-SWCNTs but from the functionalization agent, PAMAM-G0. The addition of PAMAM-G0 in epoxy can noticeably increase both tensile strength and ductility of epoxy as shown above. This improvement helps improve the fracture toughness of the epoxy/F-SWCNT system. The above explanation is evidenced by the significantly improved fracture toughness in epoxy/PAMAM-G0 than neat epoxy.

The above finding implies that PAMAM-G0 is effective in functionalization of oxidized SWCNT to achieve good dispersion and strong interfacial adhesion in epoxy. However, the improvement on the mechanical properties is still not entirely significant.

It may be required that SWCNTs be de-bundled (de-rope) and become straight in epoxy to realize the benefit of SWCNTs reinforcement in epoxy.

Surface functionalization of SWCNTs by oxidation and subsequent PAMAM-G0 functionalization appears to be effective in improving dispersion and their adhesion in epoxy matrix. This is another indication that covalent surface functionalization of SWCNTs using PAMAM-G0 is effective. However, even when SWCNTs are well dispersed and exhibit strong adhesion in epoxy matrix, the improvements in tensile properties are still limited. This suggests that significantly improved dispersion and prevention of curling may be needed to realize the potential of SWCNTs in enhancing mechanical properties of epoxy resins.

#### *Dynamic Mechanical Behavior*

The DMA testing results were shown in Figure 11 and summarized in Table 3. The  $T_g$  of the epoxy matrix is reduced slightly after the addition of either P-SWCNTs or F-SWCNTs. For epoxy/P-SWCNT, the slight drop in  $T_g$  might be due to partial absorption of the curing agent by P-SWCNT. This results in alteration of curing stoichiometric ratio, thus reducing the  $T_g$  and crosslink density of cured epoxy resin. For epoxy/F-SWCNT, the presence of excess amine groups can also cause the  $T_g$  of epoxy/F-SWCNT to drop, but not as much as that of epoxy/PAMAM-G0. For epoxy/PAMAM-G0, the participation of PAMAM-G0 in the epoxy curing reaction has led to the drop in epoxy  $T_g$  [50,51]. In short, the drop in  $T_g$  for above samples is because of unintended reactions that affect epoxy curing.

Table 3 Summary of key DMA properties

Sample	Neat Epoxy	Epoxy/ P-SWCNT	Epoxy/ F-SWCNT	Epoxy/ PAMAM-G0
Rubbery plateau modulus (MPa)	25.4	24.1	34.4	23.4
$T_g$ ( $^{\circ}\text{C}$ )	139.7	133.8	134.9	132.0

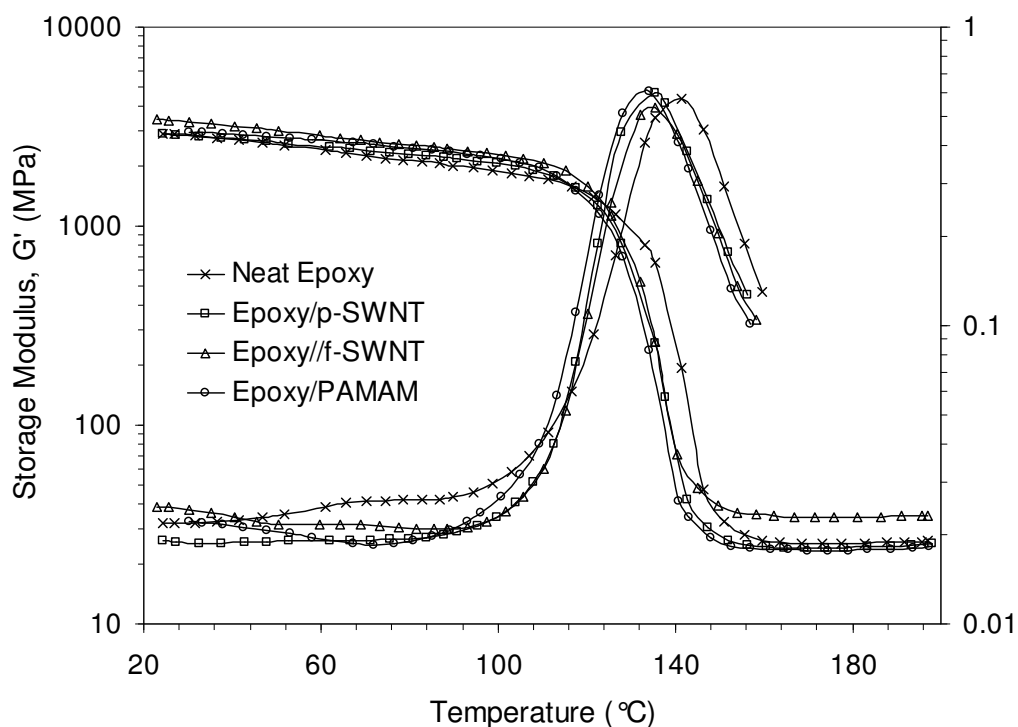


Figure 11 DMA results of epoxy/nanocomposites

It is interesting to observe that the storage moduli of the samples exhibit different degrees of improvement at temperatures above and below  $T_g$ . Above  $T_g$ , an addition of P-SWCNT or PAMAM-G0 reduces the rubbery plateau moduli. The lowered rubbery plateau modulus of epoxy/P-SWCNT is possibly due to either lower crosslink density of epoxy or poor adhesion between SWCNTs and epoxy, or both. The reduction of rubbery

plateau modulus in epoxy/PAMAM-G0 is probably because of the unintended reactions between epoxy monomer and the amine groups on PAMAM-G0 dendrimers. The rubbery plateau modulus is significantly increased for epoxy/F-SWCNT, which is believed to be due to greatly improved dispersion and adhesion with epoxy, as evidenced by SEM and TEM images.

At temperatures below  $T_g$ , the storage modulus of epoxy/F-SWCNT is still higher than epoxy/P-SWCNT, but the improvement is much smaller than that observed above  $T_g$ . Similar phenomenon has been studied by Gersappe using molecular dynamics modeling. The modeling results suggest that the ability of the nanofillers to carry and redistribute the applied stress field depends strongly on the mobility and the size of nanofiller [32]. Thus, when the nanotubes are well exfoliated and mobilized by the surrounding molecules, the stiffening effect would be maximized at temperatures above  $T_g$  and becomes greatly reduced at temperatures below  $T_g$ . Such a phenomenon has also been observed in a few other well dispersed polymer nanocomposites systems [50,52,53].

## **CHAPTER VI**

### **EFFECT OF SULFANILAMIDE AND NYLON PARTICLES ON EPOXY/SWCNT BASED NANOCOMPOSITES**

In this research, a new strategy for placing epoxy nanocomposites with high content of SWCNT and nylon particles at the location of interest by the preparation of partially cured (B-staged) epoxy/SWCNT/nylon thin films is reported. Because the films are partially cured, the SWCNT and nylon particles will be locked in place even after they are subsequently co-cured and integrated with neat epoxy within a VARTM composite. Since the thin films are prepared separately, higher SWCNT and nylon particle loadings can be incorporated in the polymer matrix without compromising processability, especially for the VARTM process. Thus, desirable properties, such as good mechanical strength and greatly increased fracture toughness can be achieved at a location of interest at much lower cost.

#### **EXPERIMENTAL**

##### *Viscosity*

Viscosity property testing of epoxy/SWCNT nanocomposites were acquired using an Anton Poar Physica MCR 300 Rheometer. The samples were tested used a parallel plate (25 mm diameter) on the controlled shear rate/shear stress sensor system from a 10-500 shear rate at log scale. The thickness of the sample was 1 mm at 70 °C to

mimic the processing temperature of the rotavapor. The rheometer was calibrated before each measurement and a thermal system was used to keep the temperature constant.

The remaining part of the experimental section here is the sum of the previous experimental sections in previous chapters. All of the same experiments are performed here to evaluate the effect sulfanilamide and nylon particles have on epoxy/SWCNT nanocomposites.

## RESULTS AND DISCUSSION

### *Background on Sulfanilamide and Nylon Particles*

The use of sulfanilamide as the new surface modifier is useful in multiple aspects. Sulfanilamide consists of a benzene ring with two different end groups. One end group is less involved while the other end group is quite bulky in nature. The structure of sulfanilamide is shown in Figure 12.

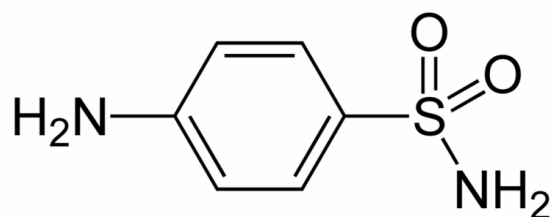


Figure 12 Chemical structure of sulfanilamide

The NH<sub>2</sub> end group melts around a temperature of 120 °C while the SO<sub>2</sub>-NH<sub>2</sub> end group melts around 165 °C. This allows for easier processing by only allowing a partial

amount of the surface modifier to react, which helps to keep the viscosity of the epoxy/nanocomposites low.

The backbone rigidity of sulfanilamide as a surface modifier/curing agent has been found to strongly influence the modulus and  $T_g$  of epoxies [54-56]. Upon toughening with nylon particles, the crosslinking between the particles is the most critical part of the toughening of epoxy. The well known correlation between toughenability and the average molecular weight between crosslinks does not necessarily hold true when the nature of epoxy backbone molecular mobility is altered [56-58].

The toughening mechanisms of epoxy/nylon nanocomposites have been extensively evaluated [59-61]. In brittle systems, where plastic deformation ahead of the crack tip is normally limited, the particles are toughened by two mechanisms: stress concentration induced by plastic deformation and particle bridging [59]. In particle bridging, the nylon particles first initiate microcracks in the interlaminar region which is shown in further SEM investigation. It has been confirmed that, in the case of unmodified resins, the thinner specimens which experienced nearly uniaxial tensile stress exhibited much higher local strains at failure than the thicker counterparts which experienced highly triaxial tensile stress [60]. While montmorillonite clay is the most common filler [61], the use of nylon as the toughening particle is growing extensively recently.

B-staged epoxy/ SWCNT nanocomposite thin films toughened by nylon particles at 50% of cure have been prepared for improving conductivity and mechanical performance of laminated composites. The SWCNTs were functionalized by oxidation

and subsequent grafting using sulfanilamide as the surface modifier. The toughened epoxy nanocomposites containing SWCNTs and nylon were successfully cast into thin films by manipulating degree of cure and viscosity of epoxy. The morphology and mechanical properties of the above toughened composite systems were investigated. It is found that surface functionalization and toughening can effectively improve the dispersion and adhesion of SWCNTs in epoxy and improve the mechanical properties and fracture toughness of the nanocomposite. The B-staged thin films can be seamlessly integrated into laminated composite systems upon heating, and can serve as interleaves for improving conductivity and mechanical strengths of laminated fiber composite systems.

#### *Addition of Sulfanilamide and Nylon Particles*

Nylon particles have been widely used as an important engineering plastic and synthetic fiber due to its excellent load bearing (strength and stiffness) capability at elevated temperature, resistance to chemical abrasions, toughness and resistance to impact, and low coefficient of friction [62-65]. Polymer nanocomposites with nylon particles offer tremendous improvement in a wide range of physical and engineering properties for polymers while at low loading [66]. Extensive studies have been performed to view the filler loading [67] and to discuss the challenges for processing, characterization and the mechanisms governing their behavior [68]. Studies on the effects of SWCNTs with nylon on epoxy nanocomposites have been evaluated [69-71]. The ideal fracture surface should show good dispersion of nylon particles and SWCNTs

which improve the mechanical performance of composites, as reflected by improved modulus and strength [70-71].

Sulfanilamide is the improved surfactant that was used to treat the surface of O-SWCNTs to form F-SWCNTs. The corresponding amount of sulfanilamide (1:1 weight ratio with SWCNT) was added to the O-SWCNT sample dispersed in acetone followed by one hour of sonication to ensure good mixing and interaction.

The nylon particles were first dispersed in acetone at a predetermined ratio to achieve a final loading of 10 wt% in epoxy. This solution was sonicated for 5 minutes to promote increased dispersion. The F-SWCNTs, which were well dispersed in acetone, were then added to the nylon and acetone solution followed by an additional 5 minutes of sonication to further promote increased dispersion. The remaining procedure is the same as previously stated. Nylon particles were added to all samples at a loading of 10 wt% to observe its effects. Also, nylon at 5 wt% was prepared for epoxy/O-SWCNT and epoxy/F-SWCNT(sulfanilamide) for comparison. A predetermined amount of the epoxy monomer was added to the solution and sonicated for 15 min. to achieve a final SWCNT loading of 0.5 wt% in the final nanocomposite.

### *Characterization*

Optical Microscopy (OM) was used to observe the effects that numerous surfactants had on SWCNT and observe how well SWCNT and nylon disperse together. PAMAM-G0 dendrimer was the previously used surfactant which produced good results in terms of dispersion and adhesion of SWCNT with epoxy and improved mechanical

properties. PAMAM-G0 is quite expensive to use which would render it not applicable for bulk processing. Amines with varying end groups were chosen as a replacement for the PAMAM-G0 dendrimer. Sulfanilamide, Jeffamine EDR-148, EDR-176 and T-403 were chosen as suitable replacements since they were readily available. Sulfanilamide was the only amine that was in solid form, and it ultimately yielded the best comparable dispersion of SWCNTs to PAMAM-G0. OM pictures taken at 10x are shown in Figure 13.

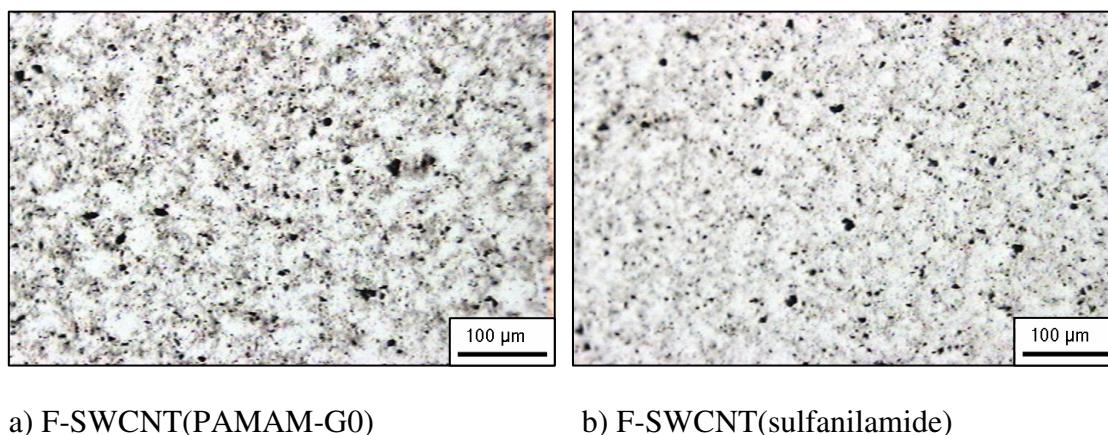


Figure 13 OM images (10x) of F-SWCNT nanocomposite samples

Sulfanilamide was found to give a slightly higher degree of dispersion when compared to the previously used PAMAM-G0 dendrimer. This higher degree of dispersion means that the mechanical properties of the new systems will achieve the same if not better material properties when compared to the older systems.

DSC was used to observe the effects on  $T_g$  that occurs when SWCNTs and nylon particles were added. The neat epoxy tested in this study had a  $T_g$  of 143.8 °C. It is

desired to maintain a  $T_g$  around that of neat epoxy for all samples in order to avoid any unwanted morphological and property changes. Table 4 lists the  $T_g$  values determined.

Table 4 Glass transition temperature ( $T_g$ ) of epoxy/SWCNT/nylon nanocomposites

Sample	$T_g$ (°C)
Neat Epoxy (Neat)	143.8
P-SWCNT	138.6
O-SWCNT	142.6
F-SWCNT(PAMAM-G0)	144.7
F-SWCNT(Sulfanilamide)	141.3

Sample	$T_g$ (°C)
Neat/Nylon (10 wt%)	144.1
P-SWCNT/Nylon (10 wt%)	140.2
O-SWCNT/Nylon (10 wt%)	142.8
F-SWCNT(Sulfanilamide)/Nylon (10 wt%)	142.6
O-SWCNT/Nylon (5 wt%)	142.9
F-SWCNT(Sulfanilamide)/Nylon (5 wt%)	142.8

It was found that the addition of P-SWCNT lowers the  $T_g$  slightly. This could be explained by the P-SWCNT essentially acting as a defect or a void in the epoxy, which would naturally lower its  $T_g$ . All other SWCNTs that were either oxidized or functionalized maintained a  $T_g$  around that of neat epoxy. The treated SWCNTs effectively bond themselves to epoxy to eliminate the effect of defects or voids contained within the nanocomposites. The addition of nylon particles with a melting point of 165 °C almost has no effect on the  $T_g$  when compared to neat epoxy. This helps to show that the addition of nylon particles shows no negative effects on the thermal properties of the epoxy/nanocomposites.

## Viscosity

Information about all of the epoxy nanocomposite viscosities is shown in Figure

14.

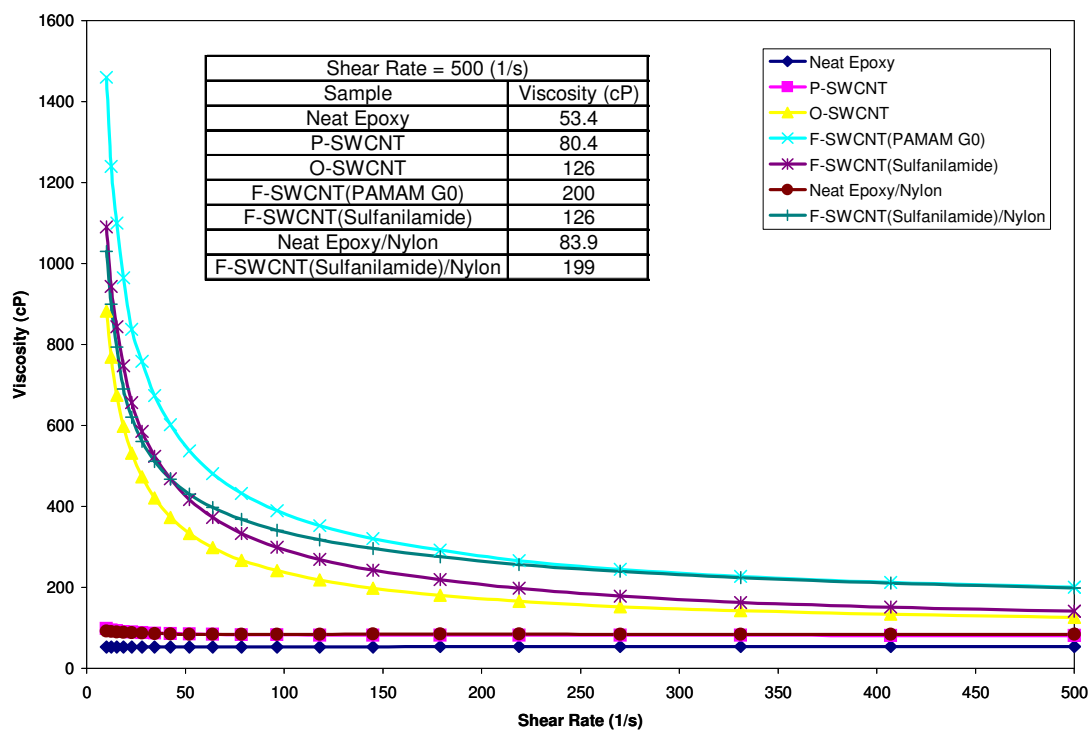


Figure 14 Viscosity vs. shear rate of epoxy/nanocomposites

The addition of SWCNT to the epoxy/nanocomposites makes the fluid behave non-Newtonian which accounts for the altering viscosities at altering shear rates. The addition of nylon keeps the epoxy/nanocomposites behaving as a Newtonian fluid. For comparison, the shear rate of 500 1/s was chosen to mimic the behavior of the casting process of the thin film coater during processing. It was observed that the addition of nylon particles to the epoxy/SWCNT nanocomposites had moderate effects on the

overall viscosity of the systems. The increase in viscosity is able to be kept under control by keeping the temperature of the film coater at 90 °C. This temperature allows for the lowest viscosity possible before reaching its B-stage cure temperature of 100 °C. This means the processability of the samples will hardly be affected even with the addition of 10 wt% nylon particles. More information regarding this will follow.

Control of the degree of cure is an important factor in the preparation of B-staged thin films. Two factors that affect the degree of cure are temperature and duration of cure. A high degree of cure will result in high viscosity, which negatively affects the thin film formation process and also limits the curing and integration of the thin films with the VaRTM process. Concerning the control of viscosity, controlling factors such as dispersion and concentration of SWCNTs, degree of cure and film coater temperature all affect the results.

### *Tensile Behavior*

Tensile testing was performed to evaluate the effect of the SWCNT treatment with sulfanilamide and the addition of nylon particles on the mechanical properties of the epoxy nanocomposites. The key tensile properties are listed in Table 5 and Table 6.

Table 5 Mechanical properties of Epoxy/SWCNT nanocomposites (0.5 wt%)

Property	Neat Epoxy	P-SWCNT	O-SWCNT	F-SWCNT(PAMAM G0)	F-SWCNT(Sulfanilamide)
Young's Modulus (Gpa)	2.77±0.01	2.84±0.05	3.17±0.01	3.21±0.15	3.21±0.16
Tensile Strength (Mpa)	60.1±5.6	74.2±0.5	76.5±3.9	82.7±3.2	88.3±0.61
Elongation (%)	3.30±0.22	1.52±0.48	2.97±0.40	4.88±1.22	5.08±0.30
K <sub>IC</sub> (MPa•m <sup>1/2</sup> )	0.65±0.03	0.77±0.03	0.81±0.08	0.93±0.04	0.86±0.08

Table 6 Mechanical properties of Epoxy/SWCNT/Nylon nanocomposites (0.5 wt%)

Property	Neat/ Nylon (10 wt%)	P-SWCNT/ Nylon (10 wt%)	O-SWCNT/ Nylon (10 wt%)	F-SWCNT(Sulfanilamide)/ Nylon (10 wt%)	O-SWCNT/ Nylon (5 wt%)	F-SWCNT(Sulfanilamide)/ Nylon (5 wt%)
Young's Modulus (Gpa)	2.61±0.13	2.73±0.16	2.79±0.10	2.98±0.09	2.88±0.06	3.05±0.08
Tensile Strength (Mpa)	78.3±1.37	80.4±1.40	84.0±1.70	77.3±0.40	79.8±0.53	87.0±1.38
Elongation (%)	7.11±0.76	2.52±0.50	5.49±0.82	5.60±0.84	5.43±0.31	5.56±0.43
K <sub>IC</sub> (MPa·m <sup>1/2</sup> )	0.95±0.09	0.99±0.07	1.02±0.10	1.12±0.09	0.94±0.05	1.02±0.07

The results show that the incorporation of P-SWCNT can improve the epoxy Young's modulus and tensile strength by 2% and 19%, respectively. Possible reasons for the limited Young's modulus and tensile strength improvements may be due to the fact that most SWCNTs are poorly dispersed and are still bundled. Only few are individually dispersed in epoxy. As a result, the reinforcement effect is compromised. The SWCNT at this stage effectively acts as a defect. Oxidation of SWCNTs leads to a much better dispersion effect and thus the mechanical properties of epoxy/O-SWCNT were further improved. The incorporation of F-SWCNTs(sulfanilamide) leads to the best overall reinforcement effect in Young's modulus and tensile strength by 14% and 32%, respectively. The tensile properties of the epoxy nanocomposite samples show a good correlation with the level of dispersion of SWCNTs in the epoxy matrix. The above study suggests that, as expected, the better the dispersion of SWCNT in epoxy results in better improvements in mechanical properties fracture toughness. The higher elongation at break for epoxy/F-SWCNT nanocomposites compared to neat epoxy signifies that the sizes of SWCNT domain are smaller than the critical flaw size for epoxy. Furthermore, the addition of sulfanilamide as a surface modifier for SWCNT might alter epoxy curing

and matrix properties to some degree. The data above are the bulk properties of the nanocomposites.

#### *Dynamic Mechanical Behavior*

The DMA testing results are shown in Figure 15. The  $T_g$  of Neat Epoxy is 145.5 °C which is similar to the DSC results. The  $T_g$  of the epoxy matrix is reduced slightly after the addition of either F-SWCNTs or nylon particles. For Neat Epoxy/Nylon, the  $T_g$  was 139 °C. This  $T_g$  is slightly lower than  $T_g$  from the DSC. This could be due to a poorly prepared DMA sample. The slight drop in  $T_g$  might be due to partial absorption of the curing agent by the nylon particles. This results in alteration of curing stoichiometric ratio, thus reducing the  $T_g$  and crosslink density of cured epoxy resin. For F-SWCNT/Nylon, the  $T_g$  was 141.2 °C which is similar to the DSC results. The presence of excess amine groups can also cause the  $T_g$  of epoxy/F-SWCNT to increase in this case by effectively increasing the amount of curing agent added.

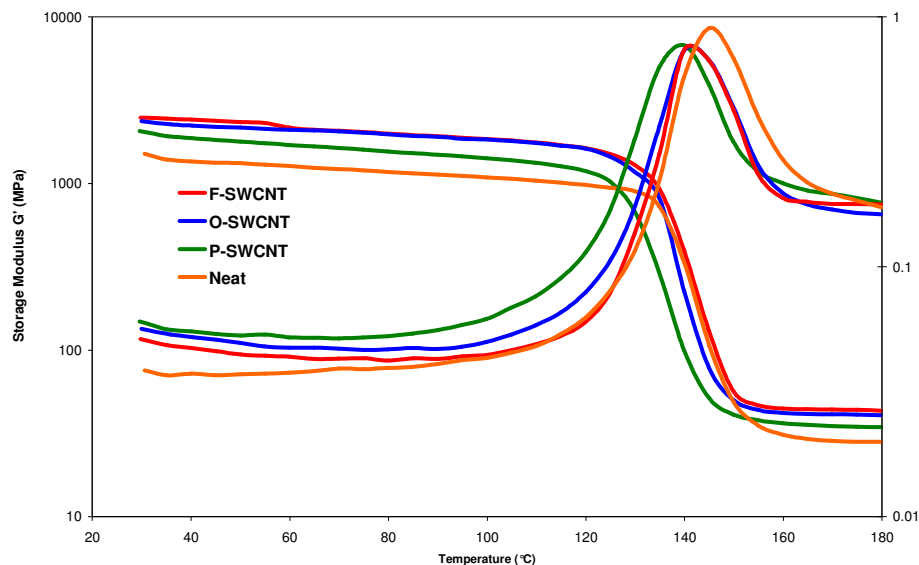
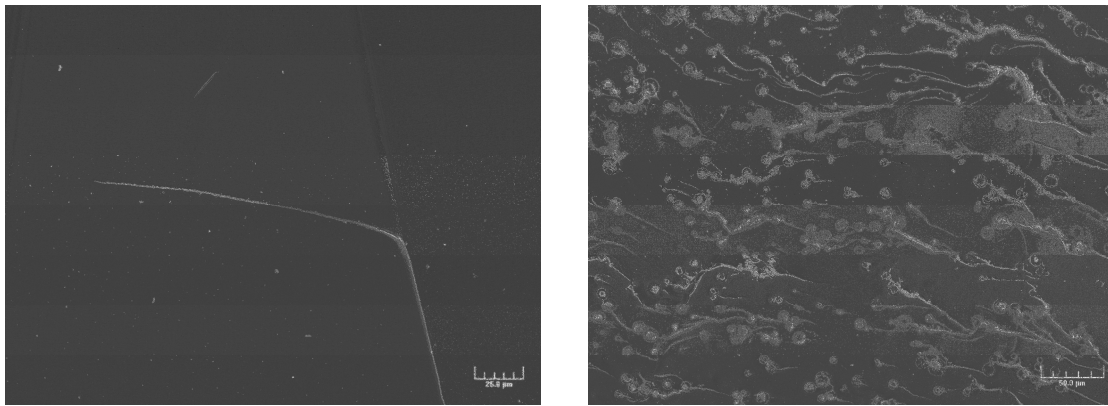


Figure 15 DMA results of epoxy/nylon nanocomposites

The addition of nylon appears to increase the rubbery plateau modulus in the case of neat epoxy and Neat/Nylon. On the other hand, the rubbery plateau modulus remains unchanged between F-SWCNT and F-SWCNT/Nylon. This could be due to the steric hindrance issues with the epoxy molecules as well as the crosslink density remaining unchanged.

### *Fracture Behavior*

SEM investigation on epoxy/SWCNT nanocomposites surfaces can clearly show the improvement on fracture toughness with the addition of SWCNTs and especially the nylon particles. The crack tip on the fracture surfaces of neat epoxy shown in Figure 16a and neat epoxy/nylon (10 wt%) in Figure 16b are shown.



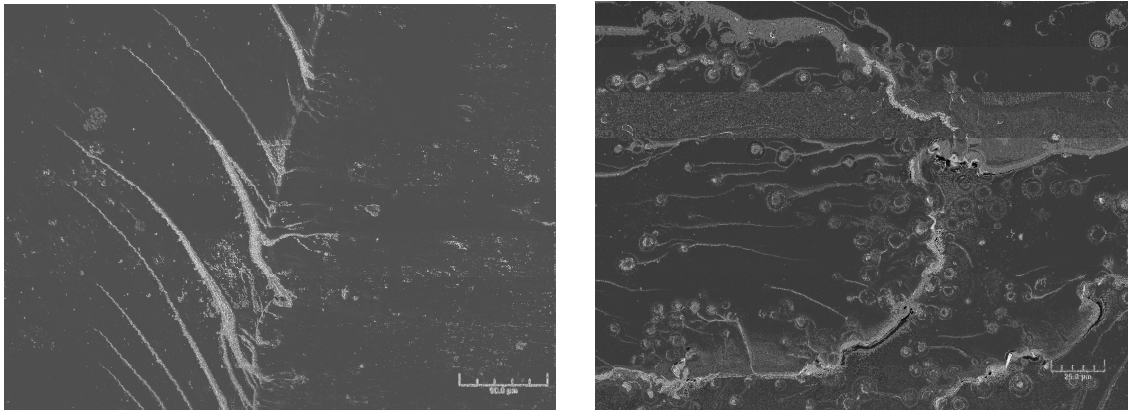
a) Neat Epoxy

b) Neat Epoxy/Nylon (10 wt%)

Figure 16 SEM images of fracture surface of neat epoxy nanocomposite samples

The crack propagation shows that neat epoxy is extremely brittle. No real deviation in crack growth is observed. With the addition of 10 wt% nylon particles, crack propagation is separated into hundreds of micro-cracks. These micro-cracks help to deflect the fracture energy towards the nylon particles to absorb a partial amount of energy. This can later be proven by the fact that the fracture toughness in neat epoxy/nylon increases by 32% over neat epoxy.

The crack tip on the fracture surfaces of F-SWCNT (Figure 17a) and F-SWCNT/nylon (10 wt%) (Figure 17b) are shown. The crack propagation forms micro-cracks that move towards areas of SWCNTs and nylon particles. It is visible that a number of micro-cracks move into nylon particles then disappear. This shows that the nylon particles are able to fully absorb micro-cracks to a degree.



a) F-SWCNT(sulfanilamide)

b) F-SWCNT(sulfanilamide)/Nylon (10 wt%)

Figure 17 SEM images of fracture surface of epoxy/F-SWCNT nanocomposite samples

This is due to the addition of SWCNTs in epoxy to help absorb the fracture energy which increases its fracture toughness by 24% over neat epoxy. The addition of nylon particles further improves the fracture toughness by 42%. F-SWCNT, with or without nylon particles, behaves the same way. The addition of sulfanilamide as the surfactant helps to further improve the overall dispersion and adhesion of SWCNTs in epoxy, which improve the mechanical and material properties even further.

The  $K_{IC}$  of the samples are listed in Table 5 and Table 6. There is only a slight difference in  $K_{IC}$  values among the neat epoxy and epoxy/P-SWCNT, which is probably because the epoxy resin is inherently brittle and SWCNTs themselves cannot effectively promote toughening mechanisms, such as shear banding and crack bridging in epoxy nanocomposites. There is an observed fracture toughness improvement in epoxy/O-SWCNT and further improvement in epoxy/F-SWCNT(PAMAM-G0) which is believed to be not from the presence of F-SWCNTs but from the functionalization agent,

PAMAM-G0. The addition of PAMAM-G0 in epoxy can noticeably increase the Young's modulus, tensile strength and elongation of epoxy. This improvement helps improve the fracture toughness of the epoxy/F-SWCNT(PAMAM-G0) system by around 30% over neat epoxy.

The use of the PAMAM-G0 dendrimer is very costly. In an effort to save a substantial amount of money for processing, sulfanilamide was used as the surfactant to compare against PAMAM-G0. With the addition of a 1:1 weight ratio of sulfanilamide to SWCNT, the overall mechanical properties of the nanocomposite behaved in generally the exact same manner. This helps to strengthen the decision to use sulfanilamide as the improved surfactant.

The addition of nylon particles to the epoxy/nanocomposite greatly improves the fracture toughness while only slightly decreasing the Young's modulus. 10 wt% nylon particles were used in all systems and 5 wt% nylon particles were used for the epoxy/O-SWCNT and epoxy/F-SWCNT(sulfanilamide) systems for comparison of the effect of nylon. The highest fracture toughness of all samples comes from the epoxy/F-SWCNT(sulfanilamide)/nylon (10 wt%) system where a 42% increase in  $K_{IC}$  is observed.

The above finding implies that sulfanilamide is effective in functionalization of oxidized SWCNT to achieve good dispersion and strong interfacial adhesion in epoxy. Furthermore, the addition of nylon particles significantly improves fracture toughness. This is due to the inherent ability of the nylon particles to absorb the energy of fracture by re-directing crack growth in nanocomposites as shown by the SEM pictures.

## CHAPTER VII

### CONCLUSIONS AND REMARKS

#### CONCLUSIONS ON EPOXY/SWCNT THIN FILM STUDY

B-staged epoxy/SWCNT nanocomposite thin films have been successfully prepared. High degree of dispersion of SWCNTs in epoxy thin films has been achieved. The SEM, TEM and Raman microscopy investigations indicate that the degree of dispersion dramatically increases as the SWCNTs are oxidized and functionalized by PAMAM-G0 dendrimers and by sulfanilamide. The use of sulfanilamide as the surfactant shows comparable mechanical and thermal properties as the previously used PAMAM-G0 dendrimer while being easier to handle and lowering the processing cost. A high degree of dispersion of SWCNTs throughout the preparation of epoxy/SWCNT nanocomposite thin films yields high quality B-staged epoxy/SWCNT nanocomposite thin films. The degree of cure for the B-staged thin films has been monitored and determined by DSC. The B-stage thin films with 50% cure give satisfactory properties for VaRTM processing to help enhance mechanical properties of the laminated composites. Additionally, a high degree of dispersion of SWCNTs and nylon particles throughout the preparation of the nanocomposite yields high quality B-staged epoxy/SWCNT/nylon nanocomposite thin films. The addition of nylon to epoxy/SWCNT nanocomposites helps to improve overall nanocomposite dispersion and dramatically improve fracture toughness while not adversely affecting  $T_g$  or viscosity. The present finding suggests that these epoxy/SWCNT/nylon nanocomposite thin films

can be easily used as interleaves for VARTM composite laminates applications for improved mechanical properties and fracture toughness.

### **RECOMMENDATIONS FOR FUTURE WORK**

An extensive amount of research has been completed for this project which is given by the Air Force Research Labs (AFRL). The preparation and processing aspect produces high quality samples that yield high quality results. The epoxy/SWCNT nanocomposite samples possess good mechanical properties, high thermal stability and high fracture toughness. Future work could be to focus more on the conductivity side of the nanocomposites. Developing an epoxy/SWCNT nanocomposites that possesses good qualities and properties is the ultimate goal. Also, more inventive applications for the use of the epoxy/SWCNT nanocomposites thin films can be sought after.

## REFERENCES

- [1] Iijima, S. *Nature* 1991, 354, 56-58.
- [2] Ebbesen, T. W. *Annual Review of Materials Science* 1994, 24, 235-264.
- [3] Bernholc, J.; Brenner, D.; Buongiorno Nardelli, M.; Meunier, V.; Roland, C. *Annual Review of Materials Research* 2002, 32, 347-375.
- [4] Terrones, M. *Annual Review of Materials Research* 2003, 33, 419-501.
- [5] Dresselhaus, M. S.; Dresselhaus, G.; Jorio, A. *Annual Review of Materials Research* 2004, 34, 247-278.
- [6] Thostenson, E. T.; Ren, Z.; Chou, T.-W. *Composites Science and Technology* 2001, 61, 1899-1912.
- [7] Yu, M.-F.; Files, B. S.; Arepalli, S.; Ruoff, R. S. *Physical Review Letters* 2000, 84, 5552-5555.
- [8] Nikolaev, P.; Bronikowski, M. J.; Bradley, R. K.; Rohmund, F.; Colbert, D. T.; Smith, K. A.; Smalley, R. E. *Chemical Physics Letters* 1999, 313, 91-97.
- [9] Thess, A.; Lee, R.; Nikolaev, P.; Dai, H.; Petit, P.; Robert, J.; Xu, C.; Lee, Y. H.; Kim, S. G.; Rinzler, A. G.; Colbert, D. T.; Scuseria, G. E.; Tomanek, D.; Fischer, J. E.; Smalley, R. E. *Science* 1996, 273, 483-487.
- [10] Hone, J.; Llaguno, M. C.; Biercuk, M. J.; Johnson, A. T.; Batlogg, B.; Benes, Z.; Fischer, J. E. *Applied Physics A: Materials Science & Processing* 2002, 74, 339-343.
- [11] Xie, X.-L.; Mai, Y.-W.; Zhou, X.-P. *Materials Science & Engineering, R: Reports* 2005, R49, 89-112.
- [12] Moniruzzaman, M.; Winey, K. I. *Macromolecules* 2006, 39, 5194-5205.
- [13] Liu, P. *European Polymer Journal* 2005, 41, 2693-2703.
- [14] Zhu, J.; Kim, J.; Peng, H.; Margrave, J. L.; Khabashesku, V. N.; Barrera, E. V. *Nano Letters* 2003, 3, 1107-1113.

- [15] Zhu, J.; Peng, H.; Rodriguez-Macias, F.; Margrave, J. L.; Khabashesku, V. N.; Imam, A. M.; Lozano, K.; Barrera, E. V. *Advanced Functional Materials* 2004, 14, 643-648.
- [16] Gong, X.; Liu, J.; Baskaran, S.; Voise, R. D.; Young, J. S. *Chemistry of Materials* 2000, 12, 1049-1052.
- [17] Bhattacharyya, A. R.; Sreekumar, T. V.; Liu, T.; Kumar, S.; Ericson, L. M.; Hauge, R. H.; Smalley, R. E. *Polymer* 2003, 44, 2373-2377.
- [18] Shofner, M. L.; Khabashesku, V. N.; Barrera, E. V. *Chemistry of Materials* 2006, 18, 906-913.
- [19] Du, F.; Scogna, R. C.; Zhou, W.; Brand, S.; Fischer, J. E.; Winey, K. I. *Macromolecules* 2004, 37, 9048-9055.
- [20] Sreekumar, T. V.; Liu, T.; Min, B. G.; Guo, H.; Kumar, S.; Hauge, R. H.; Smalley, R. E. *Advanced Materials* 2004, 16, 58-61.
- [21] Zhang, X.; Liu, T.; Sreekumar, T. V.; Kumar, S.; Moore, V. C.; Hauge, R. H.; Smalley, R. E. *Nano Letters* 2003, 3, 1285-1288.
- [22] Ajayan, P. M.; Schadler, L. S.; Giannaris, C.; Rubio, A. *Advanced Materials* 2000, 12, 750-753.
- [23] Grossiord, N.; Loos, J.; Regev, O.; Koning, C. E. *Chemistry of Materials* 2006, 18, 1089-1099.
- [24] Coleman, J. N.; Cadek, M.; Blake, R.; Nicolosi, V.; Ryan, K. P.; Belton, C.; Fonseca, A.; Nagy, J. B.; Gun'ko, Y. K.; Blau, W. J. *Advanced Functional Materials* 2004, 14, 791-798.
- [25] O'Connell, M. J.; Boul, P.; Ericson, L. M.; Huffman, C.; Wang, Y.; Haroz, E.; Kuper, C.; Tour, J.; Ausman, K. D.; Smalley, R. E. *Chemical Physics Letters* 2001, 342, 265-271.
- [26] Kang, Y.; Taton, T. A. *Journal of the American Chemical Society* 2003, 125, 5650-5651.
- [27] Shin, H.-i.; Min, B. G.; Jeong, W.; Park, C. *Macromolecular Rapid Communications* 2005, 26, 1451-1457.
- [28] Calvert, P. *Nature* 1999, 399, 210-211.

- [29] Liu, J.; Rinzler, A. G.; Dai, H.; Hafner, J. H.; Bradley, R. K.; Boul, P. J.; Lu, A.; Iverson, T.; Shelimov, K.; Huffman, C. B.; Rodriguez-Macias, F.; Shon, Y.-S.; Lee, T. R.; Colbert, D. T.; Smalley, R. E. *Science* 1998, 280, 1253-1256.
- [30] Shi, Z.; Lian, Y.; Zhou, X.; Gu, Z.; Zhang, Y.; Iijima, S.; Gong, Q.; Li, H.; Zhang, S.-L. *Chemical Communications* 2000, 461-462.
- [31] Garg, A.; Sinnott, S. B. *Chemical Physics Letters* 1998, 295, 273-278.
- [32] Sue, H. J.; Jones, R. E.; Garcia-Meitin, E. I. *Journal of Materials Science* 1993, 28, 6381-91.
- [33] Groleau, M. R.; Shi, Y. B.; Yee, A. F.; Bertram, J. L.; Sue, H. J.; Yang, P. C. *Composites Science and Technology* 1996, 56, 1223-1240.
- [34] Lee, S.-H.; Noguchi, H.; Kim, Y.-B.; Cheong, S.-K. *Journal of Composite Materials* 2002, 36, 2153-2168.
- [35] Lee, S.-H.; Noguchi, H.; Kim, Y.-B.; Cheong, S.-K. *Journal of Composite Materials* 2002, 36, 2169-2181.
- [36] Derkowski, B. J.; Sue, H.-J. *Polymer Composites* 2003, 24, 158-170.
- [37] Kishi, H.; Kuwata, M.; Matsuda, S.; Asami, T.; Murakami, A. *Composites Science and Technology* 2004, 64, 2517-2523.
- [38] Fan, Z.; Alms, J.; Advani, S. G. In *Proceedings of the 20th Annual Technical Conference American Society for Composites*, Philadelphia, PA, 2005, p 159-166.
- [39] Kim, J.; Barrera, E. V.; Armeniades, C. D. In *International SAMPE Technical Conference; Society for the Advancement of Material and Process Engineering*: Dayton, OH, 2003; Vol. 35, p 510-520.
- [40] Zhu, J.; Imam, A.; Crane, R.; Lozano, K.; Khabashesku, V. N.; Barrera, E. V. *Composites Science and Technology* 2007, 67, 1509-1517.
- [41] Xu, X.; Thwe, M. M.; Shearwood, C.; Liao, K. *Applied Physics Letters* 2002, 81, 2833-2835.
- [42] Xu, N. S.; Wu, Z. S.; Deng, S. Z.; Chen, J. *Journal of Vacuum Science & Technology, B: Microelectronics and Nanometer Structures* 2001, 19, 1370-1372.

- [43] Cao, Q.; Xia, M.-G.; Shim, M.; Rogers, J. A. *Advanced Functional Materials* 2006, 16, 2355-2362.
- [44] Aglan, A.; Allie, A.; Ludwick, A.; Koons, L. *Surface and Coatings Technology* 2007, 202, 370-378.
- [45] Sun, L.; Warren, G. L.; O'Reilly, J. Y.; Everett, W. N.; Lee, S. M.; Davis, D.; Lagoudas, D.; Sue, H. J. *Carbon* 2008, 46, 320-328.
- [46] Dresselhaus, M. S.; Eklund, P. C. *Advances in Physics* 2000, 49, 705-814.
- [47] Hadjiev, V. G.; Arepalli, S.; Nikolaev, P.; Jandl, S.; Yowell, L. *Nanotechnology* 2004, 15, 562-567.
- [48] Hadjiev, V. G.; Iliev, M. N.; Arepalli, S.; Nikolaev, P.; Files, B. S. *Applied Physics Letters* 2001, 78, 3193-3195.
- [49] Hadjiev, V. G.; Lagoudas, D. C.; Oh, E. S.; Thakre, P.; Davis, D.; Files, B. S.; Yowell, L.; Arepalli, S.; Bahr, J. L.; Tour, J. M. *Composites Science and Technology* 2005, 66, 128-136.
- [50] Sue, H. J.; Gam, K. T.; Bestaoui, N.; Spurr, N.; Clearfield, A. *Chemistry of Materials* 2004, 16, 242-249.
- [51] Triantafillidis, C. S.; LeBaron, P. C.; Pinnavaia, T. J. *Chemistry of Materials* 2002, 14, 4088-4095.
- [52] Boo, W. J.; Sun, L.; Liu, J.; Clearfield, A.; Sue, H.-J.; Mullins, M. J.; Pham, H. *Composites Science and Technology* 2007, 67, 262-269.
- [53] Boo, W. J.; Sun, L.; Liu, J.; Moghbelli, E.; Clearfield, A.; Sue, H.-J. *Journal of Polymer Science, Part B: Polymer Physics* 2007, DOI 10.1002/polb.
- [54] Su, W.-F.; Chen, K.-C.; Tseng, S.-Y.; *Journal of Applied Polymer Science* 2000, 78, 446-451.
- [55] Duann, Y.-F.; Liu, T.-M.; Cheng, K.-C.; Su, W.-F. ; *Polymer Degradation and Stability* 2004 ; 84, 305-310.
- [56] Sue, H.-J.; Puckett, P.; Bertram, J.; Walker, L.; Garcia-Meitin, E.; *Journal of Polymer Science Part B: Polymer Physics* 1999, 37, 2137-2149.
- [57] Fainleib, A.; Galy, J.; Pascault, J.-P.; Sue, H.-J.; *Materials Research Innovations* 2001; 4, 179-186.

- [58] Fainleib, A.; Galy, J.; Pascault, J.-P.; Sue, H.-J.; *Journal of Applied Polymer Science* 2001; 80, 580-591.
- [59] Groleau, M.; Shi, Y.-B.; Yee, A.-F.; Bertram, J. Sue, H.-J.; Yang, P.-C.; *Composites Science and Technology* 1996; 56, 1223-1240.
- [60] Kishi, H.; Shi, Y.-B.; Huang, J.; Yee, A.-F.; *Journal of Materials Science* 1998, 33, 3479-3488.
- [61] Maniar, K.; *Polymer-Plastics Technology and Engineering* 2004, 43, 427-443.
- [62] Robinson, E.; Douglas, E.; Mecholsky, J.; *Polymer Engineering and Science* 2004; 42, 2, 269-279.
- [63] Mark, J. E.; *Polymer Data Handbook*, Oxford University Press, New York, 1999; 180.
- [64] Saeed, K.; Park, S. Y.; *Journal of Applied Polymer Science* 2007, 106, 3729-3725.
- [65] Liu, T.; Phang, I. N.; Shen, L.; Chow, S. Y.; Zhang, W. D.; *Macromolecules* 2004, 37, 7214-7222.
- [66] Gao, F.; *Materials Today* 2004, 50-55.
- [67] Luo, Z. P.; Koo, J. H.; *Materials Letters* 2008, 62, 3493-3496.
- [68] Breuer, O.; Sundararaj, U.; *Polymer Composites* 2004, 25, 630-645.
- [69] Liu, T.; Phang, I.-Y.; Shen, L. ; Chow, S.-Y.; Zhang, W.-D.; *Macromolecules* 2004, 37, 7214-7222
- [70] Gao, J.; Zhao, B.; Itkis, M.; Bekyarova, E.; Hu, H.; Kranak, V.; Yu, A.; Haddon, R.; *Junior American Chemical Society* 2006; 128, 7492-7496.
- [71] Gao, J.; Itkis, M.; Yu, A.; Bekyarova, E.; Zhao, B.; Haddon, R.; *Junior American Chemical Society* 2005, 127, 3847-3854.

## VITA

Mr. Graham Warren received his Bachelor of Science degree in Chemical Engineering at Texas A&M University in College Station, Texas in August 2006. During his senior year, he became fascinated with the engineering and science behind polymers. Through some effort, he acquired a student worker position from his future advisor Dr. Hung-Jue Sue to help his current graduate students with their projects. Eventually, he grew accustomed to the research aspect of the work and joined Dr. Sue's group as a graduate student. As a graduate student, he focused most of his time on the research compiled in this thesis. Overall, Mr. Warren spent 3 years with Dr. Sue's group concerning the behavior of epoxy/SWCNT nanocomposite thin films for composites reinforcement. He received his Master of Science degree in Mechanical Engineering in May of 2009.

Mr. Warren's permanent address is:

3123 Texas A&M University  
Department of Mechanical Engineering  
c/o Dr. Hung-Jue Sue  
College Station, TX, 77843-3123